A stochastic model for neural progenitor dynamics in the mouse cerebral cortex

Frédérique Clément, Jules Olayé

A stochastic model for neural progenitor dynamics in the mouse cerebral cortex

Frédérique Clément* Jules Olayé†

Abstract

We have designed a stochastic model of embryonic neurogenesis in the mouse cerebral cortex, using the formalism of compound Poisson processes. The model accounts for the dynamics of different progenitor cell types and neurons. The expectation and variance of the cell number of each type are derived analytically and illustrated through numerical simulations. The effects of stochastic transition rates between cell types, and stochastic duration of the cell division cycle have been investigated sequentially. The model does not only predict the number of neurons, but also their spatial distribution into deeper and upper cortical layers. The model outputs are consistent with experimental data providing the number of neurons and intermediate progenitors according to embryonic age in control and mutant situations.

Keywords Stochastic model – Compound Poisson process – Cell dynamics – Cerebral cortex – Neurogenesis

1 Introduction

The cerebral cortex in mammals is the primary seat of cognitive functions, which are carried out by a wide variety of neuronal subtypes interconnected via complex neural circuits. The formation of the cerebral cortex requires the production of the right number of neurons of each subtype, in the right anatomical location, during a specific period of embryonic and fetal development, the period of neurogenesis, which lasts several days in mice and several months in humans [7, 22].
Once formed, the cerebral cortex (the dorsalmost area of the telencephalon) consists of two main types of neurons, the pyramidal (excitatory) neurons and the (inhibitory, less numerous) interneurons. Interneurons are generated outside the cortex and migrate into the cerebral cortex to settle at their definitive location, while pyramidal neurons directly derive from cortical neurogenesis [19]. During cortical neurogenesis, neural progenitors proliferate and produce neurons. In the mouse cortex, radial glial cells first undergo symmetric divisions, leading to the building-up of a pool of apical progenitors. At the onset of neurogenesis these cells switch to asymmetric divisions and generate intermediate progenitors and neurons. Neurogenesis is ended-up by the transformation of progenitors into non neural (glial) cells [16]. In [23], we have designed a deterministic multiscale model of structured cell populations, taking into account three cell types (apical progenitors, intermediate progenitors, neurons). Cell populations are described by non-conservative transport equations, whose unknowns are cell densities, distributed within a 1D functional domain, in which the spatial

*Université Paris Saclay, Inria, Centre Inria de Saclay, 91120 Palaiseau, France
†Institut Polytechnique de Paris, Inria, Centre de Mathématiques Appliquées, 91120 Palaiseau, France

variable is the cytological age, a marker of cell cycle progression. The durations of cell cycles are constant (constant ages at division for a given cell type, but different between types), while the frequencies of division in one mode or another vary with the course of embryonic development, and therefore are explicitly time-dependent. The integration of densities over the entire domain (or over a sub-part) provides access to macroscopic observations directly comparable to experimental data in cell kinetics (e.g. cell numbers, labeling index, mitotic index).

Although the total number of neural cells in the developing cortex is rapidly big enough to adopt a deterministic formalism, the usual way of investigating neurogenesis relies on histological slices, with a microscope field corresponding to only hundreds of cells. In addition, such observation windows can be used to monitor the different steps of neurogenesis according to the embryonic age, thanks to the columnar organization of the cortex, yet "lateral leakage" resulting from brain growth may affect the quantitative assessment of neural cells (and especially of neurons) with aging. Also, even if the differences in cell cycle duration seems to be mainly explainable by the cell type [2], there remains a variability in the cell cycle duration within a cell type. Finally, the final output of neurogenesis is not only characterized by the total number of neurons produced, but also by their distribution into upper or deeper layers, which appears to be at least partially stochastic [18]. A proper layering of the pyramidal neurons is critical for cerebral function. In particular, deeper-layer neurons are mostly corticofugal projection neurons, extending their axons to other areas in the central nervous system (e.g. thalamus or spinal cord), while most of upper-layer neurons are corticocortical projection neurons, extending their axons within the cortex [10].
Putting these points together motivated us to formulate a stochastic model, within the framework of compound Poisson processes, with time-varying, probabilistic fate decisions, possibly stochastic cell cycle durations and explicit classification of neurons into the upper or deeper layers. A stochastic process $X(t)$ is called a compound Poisson process if it can be represented by $X(t) = \sum_{i=1}^{N(t)} Y_i$, where $N(t)$ is a Poisson process and $(Y_i)_{1\leq i\leq N_t}$ are random variables independent conditionally to the sequence of arrival times $(T_k)_{k\in\mathbb{N}}$ [17]. Their main interest in queuing theory is that they can cope with simultaneously occurring events. Compound Poisson processes are regularly used in risk assessment studies, in various fields such as actuarial science or epidemiology (see for instance [15, 27]), yet one can only find a couple of instances related to mathematical biology. This is the case for radiobiology, and more precisely assessment of irradiation damages. In [21], the authors combined the concepts of primary radiation particles and secondary energy loss events to assess the total number of potentially damaging events. This study initiated a series of works applying the concept of compound Poisson processes to radiobiology issues ([20, 24] among others). In a more episodic way, the formalism of compound Poisson processes has been introduced in connection with stochastic gene expression with bursting transcription [31], neural excitability [4], analysis of mutation rates in the context of phylogenetics [13] or cancer [29]. To our knowledge, compound Poisson processes have yet not been used in the framework of cell lineage / cell dynamics to implement the notion of cell decision making as we do in this work.

The paper is organized as follows. Section 2 is dedicated to introducing the model flow chart and mathematical notations. In Section 3, we provide the main theoretical results, i.e. we compute estimates (expectation and variance) for the cell number in each cell type. We gather the numerical results in Section 4. Using the theoretical results obtained in Section 3, we first compare the original, deterministic model and the newly designed stochastic model, and then confront the model outputs

to experimental data on progenitor dynamics and neuron layering. We conclude in Section 5 by a biologically-oriented discussion.

2 Model design

2.1 Cell types and cell events

The model allows one to follow the dynamics of three cell types (see Figure 1): the IPgenic intermediate progenitors (IPP), the neurogenic progenitors (IPN) and the neurons (N). These dynamics are fueled with the asymmetric divisions of apical progenitors (AP), which occur with a time-varying frequency.

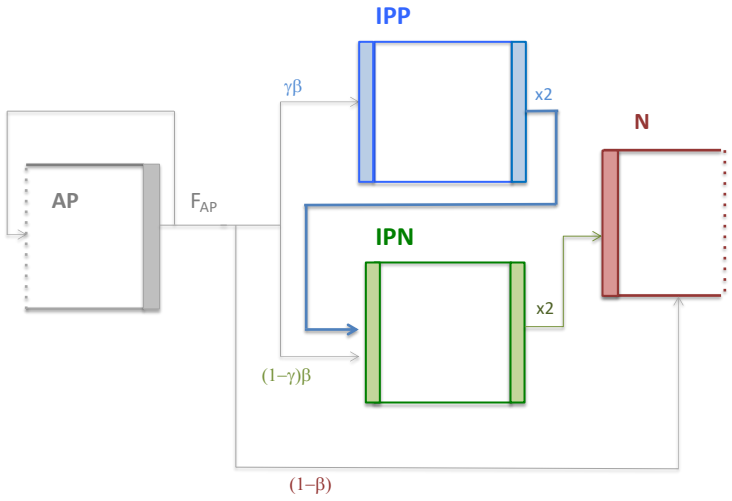

Figure 1: Cell flows in the model. *Four cell types are considered in the model : Apical Progenitors (AP), IPgenic Intermediate Progenitors (IPP), Neurogenic Intermediate Progenitors (IPN) and Neurons (N). Neurons are either generated directly from APs or indirectly from IPNs.*

At AP division onset, the cell decision making results in either direct neurogenesis (event 3 in Table 1) or indirect neurogenesis through intermediate progenitors (events 1 or 2), which amplifies the neuronal output. IPNs give rise to neurons after a single cell cycle, while IPPs cycle once before dividing as IPNs. Hence the three possible neurogenic pathways differ from the number of involved cell types, the number of neurons produced per each AP asymmetric division, and the time needed to engender neurons. More specifically, direct neurogenesis is instantaneous, while indirect neurogenesis occurs with a delay corresponding to one cell cycle duration ($T_{IPN} > 0$) for event 2, or two cycle durations ($T_{IPP} + T_{IPN}$, where $T_{IPP} > 0$) for event 1. The probability of each event is set by the time-varying rates $\beta : t \mapsto \beta(t)$ and $\gamma : t \mapsto \gamma(t)$, while the outflow of AP cells occurs at rate $F_{AP} : t \mapsto F_{AP}(t)$, where $t \in \mathbb{R}_+$.

2.2 Stochastic framework : from cell events to cell numbers

In this study, we consider that AP cell decision making is stochastic. For sake of simplicity, we first introduce and analyze the model with constant cell cycle durations. The results remain valid with

Event 1	AP	$\underset{\beta(t)\gamma(t)}{\longrightarrow}$	AP	+	IPP	$\overset{T_{IPP}}{\longrightarrow}$	2IPN	$\overset{T_{IPN}}{\longrightarrow}$	**4N**
Event 2	AP	$\underset{\beta(t)(1-\gamma(t))}{\longrightarrow}$	AP	+	IPN	$\overset{T_{IPN}}{\longrightarrow}$	**2N**		
Event 3	AP	$\underset{(1-\beta(t))}{\longrightarrow}$	AP	+	**N**				

Table 1: Different neurogenic pathways following the asymmetric division of an apical progenitor.

stochastically distributed durations (see Section 3.4 for more details). We also consider that AP asymmetric divisions occur in a probabilistic manner. To design the model, we thus need first to specify the distribution of the AP division times, and then, given that a division is occurring, to define the probability for each event to occur.

We define $\left(Z_t^{AP}\right)_{t\geq 0}$, the Poisson point process with intensity F_{AP}. For all $t \geq 0$, $Z_t^{AP} = \sum_{k\geq 1} 1_{\{T_k \leq t\}}$ counts the number of AP divisions at time t. For all $k \in \mathbb{N}^*$, T_k denotes the time of the k^{th} event (the sequence is ordered such that $(T_k)_{k\in\mathbb{N}^*}$ increases with k).
Given an arrival time T_k, another stochastic variable, Y_k, determines the "choice" of the daughter cell type. The probability that event $i_{i=\{1,2,3\}}$ occurs at T_k is given by

$$\mathbb{P}[Y_k = i \,|\, T_k] = \begin{cases} \gamma(T_k)\beta(T_k), & \text{if } i = 1, \\ (1-\gamma(T_k))\beta(T_k), & \text{if } i = 2, \\ 1-\beta(T_k), & \text{if } i = 3. \end{cases} \tag{1}$$

In Equation (1), $\beta(t)$ is the probability to engender intermediate progenitors (indirect neurogenesis, probability of events 1 and 2) when the division occurs at time $t \geq 0$. $\gamma(t)$ is the probability for an IPgenic division to give rise to an IPP (versus an IPN, event 1). The random variables $(Y_k)_{k\in\mathbb{N}^*}$ are assumed to be independent conditionally to $(T_k)_{k\in\mathbb{N}^*}$. The three events are mutually exclusive, and no other event can happen, so that $\sum_{i=1}^{3} \mathbb{P}[Y_k = i \,|\, T_k] = 1$.
From the definition of $\left(Z_t^{AP}\right)_{t\geq 0}$, we can introduce the stochastic variables counting the number of events of each type i, $i \in \{1, 2, 3\}$, at time $t \geq 0$,

$$Z_t^{(i)} = \sum_{k=1}^{Z^{AP}(t)} 1_{Y_k = i}. \tag{2}$$

For a given time $T_k \leq t \leq T_{k+1}$, one needs to know not only the numbers of past events to derive the cell number in each cell type, but also the time elapsed since the latest events 1 and 2. This is due to the delay introduced along each pathway by the cell cycle duration (see Table 1). For instance, to number the IPgenic intermediate progenitors, we have to decipher whether the IPP cell generated by the latest event 1 is still alive or, on the contrary, has already given birth to two IPN daughter cells. The same reasoning applies to the neurogenic intermediate progenitors, for which we have to decipher whether the IPN cells arisen from both latest event 1 and latest event 2 are still alive or have already differentiated into neurons.
Combining the sequence of events of each type, $(Y_k)_{k\in\mathbb{N}^*}$, with indicator functions acting as timers, we then get the formal expression of the cell number in each cell type. For all $t \geq 0$,

$$IPP(t) = \sum_{k=1}^{Z_t^{AP}} 1_{Y_k=1} 1_{t<T_k+T_{IPP}}, \tag{3}$$

$$IPN(t) = \sum_{k=1}^{Z_t^{AP}} \left(2.1_{Y_k=1} 1_{T_k+T_{IPP}\leq t<T_k+T_{IPP}+T_{IPN}} + 1_{Y_k=1} 1_{t<T_k+T_{IPN}}\right), \tag{4}$$

$$N(t) = \sum_{k=1}^{Z_t^{AP}} \left(4.1_{Y_k=1} 1_{T_k+T_{IPP}+T_{IPN}\leq t} + 2.1_{Y_k=2} 1_{T_k+T_{IPN}\leq t} + 1_{Y_k=3}\right). \tag{5}$$

It is worth noting that Equations (3)-(5) embed an explicit time-dependence, through the "conditionning" introduced by the indicator functions.

2.3 Extension to neural layering

New-born neurons settle in cortical layers in a merely inside-first outside-last pattern, with the elder neurons ending in the deeper layers and the younger in the upper ones. This patterning is yet not fully deterministic [18]. In the same spirit as in [12], we thus considered a probabilistic layer choice function, $\Delta : t \mapsto \Delta(t)$, where $t \in \mathbb{R}_+$, in which the probability to settle in the deeper layers decreases with neuron birth date

$$\begin{aligned} \Delta(t) &= \mathbb{P}[\text{New-born N} \in \text{DL} \,|\, \text{birth} = t] \\ &= \Delta_1 + \frac{\Delta_0 - \Delta_1}{\left(1 + e^{s_\Delta (t - t_\Delta)}\right)}, \end{aligned} \tag{6}$$

where $(\Delta_0, \Delta_1, s_\Delta, t_\Delta) \in [0,1]^2 \times (\mathbb{R}_+)^2$ and $\Delta_0 > \Delta_1$.
For each neuron, the birth age is computed from the time of commitment into one of the three possible AP lineages, and the subsequent (possibly stochastic) cell cycle durations of all cell types encountered in the lineage. Given the birth age and function Δ, we can distinguish the deeper layer neurons (DL) from the upper layer neurons (UL), and get, for all $t \geq 0$,

$$DL(t) = \sum_{k=1}^{Z_t^{AP}} \left(1_{Y_k=1} 1_{T_k+T_{IPP}+T_{IPN}\leq t} B_k^{(1)} + 1_{Y_k=2} 1_{T_k+T_{IPN}\leq t} B_k^{(2)} + 1_{Y_k=3} B_k^{(3)}\right), \tag{7}$$

$$UL(t) = N(t) - DL(t), \tag{8}$$

where, $(B_k^i)_{k\in\mathbb{N}^*, i\in\{1,2,3\}}$ are stochastic variables, independent conditionally to $(T_k)_{k\in\mathbb{N}^*}$ and independent of $(Y_k)_{k\in\mathbb{N}^*}$ conditionally to $(T_k)_{k\in\mathbb{N}^*}$, such that, for all $k \in \mathbb{N}^*$,

$$\begin{aligned} B_k^{(1)} | T_k &= \text{Binom}(4, \Delta(T_k + T_{IPP} + T_{IPN})), \\ B_k^{(2)} | T_k &= \text{Binom}(2, \Delta(T_k + T_{IPN})), \\ B_k^{(3)} | T_k &= \text{Binom}(1, \Delta(T_k)). \end{aligned} \tag{9}$$

2.4 Extension to stochastic cell cycle durations

Cell cycle durations, as well as the durations of the different phases of the cell cycle, vary according to the cell type [2]. In [23], we accounted for the differences in the cell cycle of IPgenic intermediate progenitors (IPPs) versus neurogenic intermediate progenitors (IPNs).
Beyond such an inter-type variability, there might be a significant intra-type variability on the scale of individual cells. The stochastic framework is well suited for studying such a variability.
We thus introduce two probability measures μ_{IPP} and μ_{IPN}, used to describe respectively the distribution of the cell cycle of IPPs and IPNs, and the following random variables:

- A sequence of independent identically distributed random variables $(S_k)_{k\in\mathbb{N}^*}$, independent of $(T_k)_{k\in\mathbb{N}^*}$, independent of $(Y_k)_{k\in\mathbb{N}^*}$, and distributed according to μ_{IPP},

- Two sequences of independent identically distributed random variables $(R_k^{(1,i)})_{k\in\mathbb{N}^*,i\in\{1,2\}}$, and $(R_k^{(2)})_{k\in\mathbb{N}^*}$. Each of these sequences are independent of $(T_k)_{k\in\mathbb{N}^*}$, $(Y_k)_{k\in\mathbb{N}^*}$, $(S_k)_{k\in\mathbb{N}^*}$, and each random variable of these sequences is distributed according to μ_{IPN}. For all $i \in \{1,2\}^2$, $(R_k^{(1,i)})_{k\in\mathbb{N}^*}$ is independent of $(R_k^{(2)})_{k\in\mathbb{N}^*}$.

- For all $i \in \{1,2\}$, a sequence of random variables $(B_k^{(1,i)})_{k\in\mathbb{N}^*}$, independent conditionally to $(T_k)_{k\in\mathbb{N}^*}$, $(R_k^{(1,i)})_{k\in\mathbb{N}^*}$, $(S_k)_{k\in\mathbb{N}^*}$, and independent of $(Y_k)_{k\in\mathbb{N}^*}$ conditionally to $(T_k)_{k\in\mathbb{N}^*}$, such that for $k \in \mathbb{N}^*$,
$$B_k^{(1,i)}|T_k, R_k^{(1,i)}, S_k = \text{Binom}(2, \Delta(T_k + S_k + R_k^{(1,i)})).$$
The sequences $(B_k^{(1,1)})_{k\in\mathbb{N}^*}$ and $(B_k^{(1,2)})_{k\in\mathbb{N}^*}$ are independent conditionally to $(T_k)_{k\in\mathbb{N}^*}$. For all $i \in \{1,2\}$, $(B_k^{(1,i)})_{k\in\mathbb{N}^*}$ is independent of $(R_k^{(1,3-i)})_{k\in\mathbb{N}^*}$.

- A sequence of random variables $(B_k^{(2)})_{k\in\mathbb{N}^*}$, independent conditionally to $(T_k)_{k\in\mathbb{N}^*}$, $(R_k^{(2)})_{k\in\mathbb{N}^*}$ and independent of $(Y_k)_{k\in\mathbb{N}^*}$ and $(B_k^{(1,i)})_{k\in\mathbb{N}^*,i\in\{1,2\}}$ conditionally to $(T_k)_{k\in\mathbb{N}^*}$, such that for $k \in \mathbb{N}^*$,
$$B_k^{(2)}|T_k, R_k^{(2)} = \text{Binom}(2, \Delta(T_k + R_k^{(2)})),$$

- A sequence of random variables $(B_k^{(3)})_{k\in\mathbb{N}^*}$, independent conditionally to $(T_k)_{k\in\mathbb{N}^*}$, and independent of $(Y_k)_{k\in\mathbb{N}^*}$, $(B_k^{(1,i)})_{k\in\mathbb{N}^*,i\in\{1,2\}}$, $(B_k^{(2)})_{k\in\mathbb{N}^*}$ conditionally to $(T_k)_{k\in\mathbb{N}^*}$, such that for $k \in \mathbb{N}^*$,
$$B_k^{(3)}|T_k = \text{Binom}(1, \Delta(T_k)).$$

From these random variables, we can write the evolution of each cell type. For all $t \geq 0$,

$$IPP(t) = \sum_{k=1}^{Z_t^{AP}} 1_{Y_k=1} 1_{t<T_k+S_k}, \tag{10}$$

$$IPN(t) = \sum_{k=1}^{Z_t^{AP}} \left(1_{Y_k=1}\left(1_{T_k+S_k\leq t<T_k+S_k+R_k^{(1,1)}} + 1_{T_k+S_k\leq t<T_k+S_k+R_k^{(1,2)}}\right) + 1_{Y_k=2} 1_{t<T_k+R_k^{(2)}}\right), \tag{11}$$

$$N(t) = \sum_{k=1}^{Z_t^{AP}} \left(1_{Y_k=1}\left(2.1_{T_k+S_k+R_k^{(1,1)}\leq t} + 2.1_{T_k+S_k+R_k^{(1,2)}\leq t}\right) + 2.1_{Y_k=2} 1_{T_k+R_k^{(2)}\leq t} + 1_{Y_k=3}\right), \tag{12}$$

$$\begin{aligned} DL(t) = \sum_{k=1}^{Z_t^{AP}} &\left(1_{Y_k=1}\left(B_k^{(1,1)}.1_{T_k+S_k+R_k^{(1,1)}\leq t} + B_k^{(1,2)}.1_{T_k+S_k+R_k^{(1,2)}\leq t}\right)\right. \\ &\left. + B_k^{(2)}.1_{Y_k=2} 1_{T_k+R_k^{(2)}\leq t} + B_k^{(3)}.1_{Y_k=3}\right), \end{aligned} \tag{13}$$

$$UL(t) = N(t) - DL(t). \tag{14}$$

3 Model analysis

In this section, we derive the theoretical expectation and variance of the cell number for each cell type. We start from the available results on compound Poisson processes with a constant intensity, and extend them to the case of time-varying intensity. We also introduce complementary technical consideration to handle the case of a stochastic cell cycle duration, which results in time-dependent stochastic kernels. Then we exploit this result to derive the first- and second-order moments for the cell number in each cell type.

3.1 Non-homogenous compound Poisson process with time-dependent stochastic kernel

Definition 1. *A compound Poisson process with intensity $\lambda : \mathbb{R}^+ \longrightarrow \mathbb{R}^+$ is a counting process $(Z_t)_{t\geq 0}$ meeting the following conditions:*

- $Z_0 = 0$,
- $(Z_t)_{t\geq 0}$ *has independent increments,*
- *for all $t \geq 0$, $h \geq 0$: $\mathbb{P}[Z_{t+h} - Z_t = 1] = \lambda(t)h + o(h)$,*
- *for all $t \geq 0$, $h \geq 0$: $\mathbb{P}[Z_{t+h} - Z_t \geq 2] = o(h)$.*

Definition 2. *Let $(Z_t)_{t\geq 0}$ be a non-homogenous Poisson process with intensity $\lambda : \mathbb{R}^+ \longrightarrow \mathbb{R}^+$. Denote $(T_n)_{n\in\mathbb{N}^*}$ the arrival times associated with Z_t. Let $(Y_t^{(n)})_{t\geq 0, n\in\mathbb{N}^*}$ be stochastic variables, defined on the same probability space, taking values in $\mathbb{R}^d$, $d \geq 1$, such that for all $t \geq 0$, $n \in \mathbb{N}^*$ and all $B_1, B_2, \ldots B_n$ Borel sets*

$$\mathbb{P}[Y_t^{(1)} \in B_1, Y_t^{(2)} \in B_2, \ldots, Y_t^{(n)} \in B_n | T_1, T_2, \ldots T_n] = \prod_{i=1}^{n} L_t(T_i, B_i),$$

where L_t is a probability kernel on $\mathbb{R}^+ \times \mathcal{B}$ ($\mathcal{B}$ is the Borel algebra). Then the process $(X_t)_{t\geq 0}$, such that, for all $t \geq 0$,

$$X_t = \sum_{k=1}^{Z_t} Y_t^{(k)}$$

is called a non-homogenous compound Poisson process. This process is characterized by its intensity $\lambda : \mathbb{R}^+ \longrightarrow \mathbb{R}^+$ and stochastic kernel $(L_t)_{t\geq 0}$.

Remark 1. *When the stochastic kernel does not depend on time, we just use L as notation.*

To handle the nonstationarity introduced by the timer (indicator) functions, we introduce the following technical definition.

Definition 3. *Let $(X_t)_{t\geq 0}$ be a non-homogenous compound Poisson process, taking its values in $\mathbb{R}^2$ ($\forall t \geq 0$, $X_t = (X_t^{(1)}, X_t^{(2)})$), with intensity $\lambda : \mathbb{R}^+ \longrightarrow \mathbb{R}^+$, and stochastic kernel $(L_t)_{t\geq 0}$. For all $t \geq 0$, $k \in \mathbb{N}^*$, we denote $Y_t^{(k,1)}$ and $Y_t^{(k,2)}$ the random variables such that*

$$X_t = \sum_{k=1}^{Z_t} \left(Y_t^{(k,1)}, Y_t^{(k,2)} \right).$$

We say that the compound Poisson process is extendable to different times, if for all $n \in \mathbb{N}^*$, $B_1, B_2, \dots B_n$ Borel sets in $\mathbb{R}^2$, $t_1, t_2 \geq 0$

$$\mathbb{P}\left[\left(Y_{t_1}^{(1,1)}, Y_{t_2}^{(1,2)} \right) \in B_1, \left(Y_{t_1}^{(2,1)}, Y_{t_2}^{(2,2)} \right) \in B_2, \dots, \left(Y_{t_1}^{(n,1)}, Y_{t_2}^{(n,2)} \right) \in B_n | T_1, T_2, \dots T_n \right] = \prod_{i=1}^{n} L_{t_1,t_2}(T_k, B_i),$$

where, for all $s \geq 0$, B a Borel set in $\mathbb{R}^2$, $L_{t_1,t_2}(s, B) = \mathbb{P}\left[\left(Y_{t_1}^{(1,1)}, Y_{t_2}^{(1,2)} \right) \in B \,|\, T_1 = s \right]$.

Remark 2. *Definition 3 means that for all $t_1, t_2 > 0$, the random variables $\left(Y_{t_1}^{(k,1)}, Y_{t_2}^{(k,2)} \right)_{k\in\mathbb{N}^*}$ remain mutually independent conditionally to $(T_k)_{k\in\mathbb{N}^*}$, and that their distributions remain well-defined by a stochastic kernel.*

We can get the characteristic function for all $t \geq 0$, and then useful information on the associated probability law, including the expectation and variance.

Theorem 1. *Let $(X_t)_{t\geq 0}$ be a non-homogenous compound Poisson process, taking its values in $\mathbb{R}^d$, $d \geq 1$, with intensity $\lambda : \mathbb{R}^+ \longrightarrow \mathbb{R}^+$, and stochastic kernel $(L_t)_{t\geq 0}$. Then, for all $t \geq 0$, $u \in \mathbb{R}^d$, the characteristic function of X_t reads*

$$\mathbb{E}\left[e^{i\langle u, X_t \rangle} \right] = \exp\left(\int_0^t \int_{\mathbb{R}^d} \left(e^{i\langle u, y \rangle} - 1 \right) L_t(s, dy) \lambda(s) ds \right).$$

The proof of Theorem 1 is a direct adaptation of that provided in [5]. It is given in the Appendix (see Section 6.1).

Corollary 1. *Let $(X_t)_{t\geq 0}$ be a non-homogenous compound Poisson process, taking its values in $\mathbb{R}$, with intensity $\lambda : \mathbb{R}^+ \longrightarrow \mathbb{R}^+$, and stochastic kernel $(L_t)_{t\geq 0}$. Then, for all $t \geq 0$*

$$\mathbb{E}[X_t] = \int_0^t \int_{\mathbb{R}} y L_t(s, dy)\lambda(s)ds,$$
$$\mathrm{Var}(X_t) = \int_0^t \int_{\mathbb{R}} y^2 L_t(s, dy)\lambda(s)ds.$$

Proof. We denote φ_t the characteristic function of X_t for all $t \geq 0$. We compute the first two derivatives of the characteristic function. For all $u \in \mathbb{R}$

$$\varphi_t'(u) = i\left(\int_0^t \int_{\mathbb{R}} y e^{iuy} L_t(s, dy)\lambda(s)ds\right) \exp\left(\int_0^t \int_{\mathbb{R}} \left(e^{iuy} - 1\right) L_t(s, dy)\lambda(s)ds\right)$$
$$\varphi_t''(u) = -\left(\int_0^t \int_{\mathbb{R}} y e^{iuy} L_t(s, dy)\lambda(s)ds\right)^2 \exp\left(\int_0^t \int_{\mathbb{R}} \left(e^{iuy} - 1\right) L_t(s, dy)\lambda(s)ds\right)$$
$$- \left(\int_0^t \int_{\mathbb{R}} y^2 e^{iuy} L_t(s, dy)\lambda(s)ds\right) \exp\left(\int_0^t \int_{\mathbb{R}} \left(e^{iuy} - 1\right) L_t(s, dy)\lambda(s)ds\right),$$

and deduce $\mathbb{E}[X_t]$ and $\mathrm{Var}(X_t)$ from the following relations

$$\mathbb{E}[X_t] = \frac{1}{i}\varphi_t'(0),$$
$$\mathrm{Var}(X_t) = \left(\varphi_t'(0)\right)^2 - \varphi_t''(0).$$

□

Corollary 2. *Let $(X_t)_{t\geq 0}$ be a non-homogenous compound Poisson process, taking its values in $\mathbb{R}^2$, extendable to different times, with intensity $\lambda : \mathbb{R}^+ \longrightarrow \mathbb{R}^+$, and stochastic kernel $(L_t)_{t\geq 0}$. We also assume that, for all $s, t_1, t_2 \geq 0$,*

$$L_{t_1,t_2}\left(s, (\mathbb{R} \times \{0\}) \cup (\{0\} \times \mathbb{R})\right) = 1.$$

Then, for all $t_1, t_2 \geq 0$ the stochastic variables $X_{t_1}^{(1)}$ and $X_{t_2}^{(2)}$ are independent.

Remark 3. *When the stochastic kernel $(L_t)_{t\geq 0}$ does not depend on time, we only need to prove that $L(s, (\mathbb{R} \times \{0\}) \cup (\{0\} \times \mathbb{R})) = 1$, for all $s \geq 0$.*

Remark 4. *The condition that $L_{t_1,t_2}\left(s, (\mathbb{R} \times \{0\}) \cup (\{0\} \times \mathbb{R})\right) = 1$ amounts to considering that the pairs of stochastic variables $(Y_{t_1}^{(k,1)}, Y_{t_2}^{(k,2)})$ take their values in $(\mathbb{R} \times \{0\}) \cup (\{0\} \times \mathbb{R})$.*

Proof. Let t_1, $t_2 \geq 0$. We prove Corollary 2 for $t_2 \geq t_1$, the proof for $t_1 \geq t_2$ is similar. We consider $(\overline{X}_t)_{t\geq 0}$ the stochastic process such that, for all $t \geq 0$,

$$\overline{X}_t = \sum_{k=1}^{Z_t} \left(Y_{\min(t,t_1)}^{(k,1)} 1_{T_k \leq t_1}, Y_t^{(k,2)}\right) = \left(X_{\min(t,t_1)}^{(1)}, X_t^{(2)}\right). \tag{15}$$

One can see that $(\overline{X}_t)_{t\geq 0}$ is a compound Poisson process with intensity λ, and stochastic kernel $(\overline{L}_t)_{t\geq 0}$, such that, for all $t, s \geq 0$ and $B_1 \times B_2$ a Borel set in $\mathbb{R}^2$

$$\begin{aligned}\overline{L}_t\left(s, B_1 \times B_2\right) &= \mathbb{P}\left[\left(Y^{(1,1)}_{\min(t,t_1)} 1_{T_1 \leq t_1}, Y^{(1,2)}_t\right) \in B_1 \times B_2 \,|\, T_1 = s\right] \\ &= \begin{cases} L_t\left(s, B_1 \times B_2\right), & \text{if } s \leq t_1,\ t < t_1, \\ L_{t_1,t}(s, B_1 \times B_2), & \text{if } s \leq t_1,\ t \geq t_1, \\ L_t(s, \mathbb{R} \times B_2) 1_{0 \in B_1}, & \text{otherwise.} \end{cases}\end{aligned}$$

For $u = (u_1, u_2)$, applying Theorem 1, and using first that $\overline{L}_{t_2}\left(s, (\mathbb{R} \times \{0\}) \cup (\{0\} \times \mathbb{R})\right) = 1$ for all $s \geq 0$ (for all $t \geq 0$ we have $L_{t,t} = L_t$, so $L_t\left((\mathbb{R} \times \{0\}) \cup (\{0\} \times \mathbb{R})\right) = 1$), and then that $e^{ix} - 1 = 0$ when $x = 0$, we get

$$\begin{aligned}\mathbb{E}\left[e^{i\langle \overline{X}_{t_2}, u\rangle}\right] &= \exp\left(\int_0^{t_2} \int_{\mathbb{R}^2} \left(e^{i\langle u, y\rangle} - 1\right) \overline{L}_{t_2}(s, dy) \lambda(s) ds\right) \\ &= \exp\left(\int_0^{t_2} \left[\int_{\mathbb{R} \times \{0\}} \left(e^{iu_1 y_1} - 1\right) \overline{L}_{t_2}(s, dy) + \int_{\{0\} \times \mathbb{R}^*} \left(e^{iu_2 y_2} - 1\right) \overline{L}_{t_2}(s, dy)\right] \lambda(s) ds\right).\end{aligned}$$

This implies, using the identity $\exp(a + b) = \exp(a)\exp(b)$,

$$\begin{aligned}\mathbb{E}\left[e^{i\langle \overline{X}_{t_2}, u\rangle}\right] &= \exp\left(\int_0^{t_2} \int_{\mathbb{R} \times \{0\}} \left(e^{iu_1 y_1} - 1\right) \overline{L}_{t_2}(s, dy) \lambda(s) ds\right) \\ &\quad \times \exp\left(\int_0^{t_2} \int_{\{0\} \times \mathbb{R}^*} \left(e^{iu_2 y_2} - 1\right) \overline{L}_{t_2}(s, dy) \lambda(s) ds\right).\end{aligned}$$

Applying the same steps as above in the reverse order, we obtain

$$\begin{aligned}\mathbb{E}\left[e^{i\langle \overline{X}_{t_2}, u\rangle}\right] &= \exp\left(\int_0^{t_2} \int_{(\mathbb{R} \times \{0\}) \cup (\{0\} \times \mathbb{R})} \left(e^{iu_1 y_1} - 1\right) \overline{L}_{t_2}(s, dy) \lambda(s) ds\right) \\ &\quad \times \exp\left(\int_0^{t_2} \int_{(\mathbb{R} \times \{0\}) \cup (\{0\} \times \mathbb{R})} \left(e^{iu_2 y_2} - 1\right) \overline{L}_{t_2}(s, dy) \lambda(s) ds\right) \\ &= \exp\left(\int_0^{t_2} \int_{\mathbb{R}^2} \left(e^{iu_1 y_1} - 1\right) \overline{L}_{t_2}(s, dy) \lambda(s) ds\right) \exp\left(\int_0^{t_2} \int_{\mathbb{R}^2} \left(e^{iu_2 y_2} - 1\right) \overline{L}_{t_2}(s, dy) \lambda(s) ds\right) \\ &= \mathbb{E}\left[e^{i\overline{X}^{(1)}_{t_2} u_1}\right] \mathbb{E}\left[e^{i\overline{X}^{(2)}_{t_2} u_2}\right].\end{aligned} \tag{16}$$

According to (15), and given that $t_2 \geq t_1$, we have $\overline{X}^{(1)}_{t_2} = X^{(1)}_{t_1}$ and $\overline{X}^{(2)}_{t_2} = X^{(2)}_{t_2}$. Combined with Equation (16), these equalities yield that $\mathbb{E}\left[e^{iu_1 X^{(1)}_{t_1} + u_2 X^{(2)}_{t_2}}\right] = \mathbb{E}\left[e^{iX^{(1)}_{t_1} u_1}\right] \mathbb{E}\left[e^{iX^{(2)}_{t_2} u_2}\right]$. By Kac's theorem (Theorem 2.1 on page 6 of [1]), we get that the stochastic variables $X^{(1)}_{t_1}$ and $X^{(2)}_{t_2}$ are independent. □

3.2 Application to progenitor dynamics

We now derive the expectation and variance for the number of intermediate progenitors (Equations (3)-(4)) in the case of constant cell cycle durations. Since the total number of neurons is fully determined by the progenitor dynamics, we also deal with the whole neuron population (Equations (5)).

We recall that $Z_t^{(i)}$ in Equation (2) is the stochastic variable counting the number of events of each type i, $i \in \{1, 2, 3\}$, at time $t \geq 0$.

Lemma 1. *For all $t \geq 0$,*

$$\begin{aligned}
\mathbb{E}[Z_t^{(1)}] &= \int_0^t \gamma(s)\beta(s)F_{AP}(s)ds, \\
\mathbb{E}[Z_t^{(2)}] &= \int_0^t (1-\gamma(s))\beta(s)F_{AP}(s)ds, \\
\mathbb{E}[Z_t^{(3)}] &= \int_0^t (1-\beta(s))F_{AP}(s)ds,
\end{aligned}$$

and

$$\begin{aligned}
\mathrm{Var}(Z_t^{(1)}) &= \int_0^t \gamma(s)\beta(s)F_{AP}(s)ds, \\
\mathrm{Var}(Z_t^{(2)}) &= \int_0^t (1-\gamma(s))\beta(s)F_{AP}(s)ds, \\
\mathrm{Var}(Z_t^{(3)}) &= \int_0^t (1-\beta(s))F_{AP}(s)ds.
\end{aligned}$$

Proof. From Equation (1), $(Z_t^{(1)})_{t\geq 0}$ is a non-homogenous compound process whose kernel reads

$$L^{(1)}(t, dy) = \gamma(t)\beta(t)\delta_1(dy) + (1-\gamma(t)\beta(t))\delta_0(dy),$$

with intensity $F_{AP} : \mathbb{R}^+ \longrightarrow \mathbb{R}^+$.
Applying Corollary 1 we have, for all $t \geq 0$,

$$\begin{aligned}
\mathbb{E}[Z_t^{(1)}] &= \int_0^t \left(\int_{\mathbb{R}} yL(s, dy) \right) F_{AP}(s)ds \\
&= \int_0^t \left((\gamma(s)\beta(s)) .1 + (1-\gamma(s)\beta(s)) .0 \right) F_{AP}(s)ds \\
&= \int_0^t \gamma(s)\beta(s)F_{AP}(s)ds,
\end{aligned}$$

and

$$\begin{aligned}
\mathrm{Var}(Z_t^{(1)}) &= \int_0^t \left(\int_{\mathbb{R}} y^2 L(s, dy) \right) F_{AP}(s)ds \\
&= \int_0^t \left((\gamma(s)\beta(s)) .1^2 + (1-\gamma(s)\beta(s)) .0^2 \right) F_{AP}(s)ds \\
&= \int_0^t \gamma(s)\beta(s)F_{AP}(s)ds.
\end{aligned}$$

Following the same reasoning, we get the result on $\mathbb{E}[Z_t^{(2)}]$, $\mathbb{E}[Z_t^{(3)}]$ and $\mathrm{Var}(Z_t^{(2)}), \mathrm{Var}(Z_t^{(3)})$, which ends the proof. □

We now derive the expectations and variances of the cell numbers. Let us consider $t \geq 0$. We begin with the simplest expressions related to neurons. Equation (5) can also be written as

$$N_t = 4Z^{(1)}_{t-T_{IPP}-T_{IPN}} 1_{t \geq T_{IPP}+T_{IPN}} + 2Z^{(2)}_{t-T_{IPN}} 1_{t \geq T_{IPN}} + Z_t^{(3)},$$

from which we deduce that

$$\mathbb{E}[N_t] = 4\mathbb{E}[Z^{(1)}_{t-T_{IPP}-T_{IPN}}] 1_{t \geq T_{IPP}+T_{IPN}} + 2\mathbb{E}[Z^{(2)}_{t-T_{IPN}}] 1_{t \geq T_{IPN}} + \mathbb{E}[Z_t^{(3)}],$$

and

$$\mathrm{Var}(N_t) = \mathrm{Var}\left(4Z^{(1)}_{t-T_{IPP}-T_{IPN}} 1_{t \geq T_{IPP}+T_{IPN}} + 2Z^{(2)}_{t-T_{IPN}} 1_{t \geq T_{IPN}} + Z_t^{(3)}\right).$$

For the variance, we use in addition the result of Corollary 2 to remove the (zero) covariance terms. Indeed, for all $(i,j) \in \{1,2,3\}^2$ such that $i \neq j$, the compound Poisson process $(Z_t^{(i)}, Z_t^{(j)})_{t \geq 0}$ has a time-independent stochastic kernel L satisfying $L(s, (\mathbb{R} \times \{0\}) \cup (\{0\} \times \mathbb{R})) = 1$ for all $s \geq 0$. We get

$$\mathrm{Var}(N_t) = 16\mathrm{Var}\left(Z^{(1)}_{t-T_{IPP}-T_{IPN}}\right) 1_{t \geq T_{IPP}+T_{IPN}} + 4\mathrm{Var}\left(Z^{(2)}_{t-T_{IPN}}\right) 1_{t \geq T_{IPN}} + \mathrm{Var}\left(Z_t^{(3)}\right).$$

Now, applying Lemma 1 gives directly the expectation and variance of the number of neurons.

Proposition 1. *For all $t \geq 0$,*

$$\begin{aligned}
\mathbb{E}[N_t] &= 4\left(\int_0^{t-T_{IPP}-T_{IPN}} \gamma(s)\beta(s)F_{AP}(s)ds\right) 1_{t \geq T_{IPP}+T_{IPN}} \\
&\quad + 2\left(\int_0^{t-T_{IPN}} (1-\gamma(s))\,\beta(s)F_{AP}(s)ds\right) 1_{t \geq T_{IPN}} \\
&\quad + \int_0^t (1-\beta(s))\,F_{AP}(s)ds, \\
\mathrm{Var}(N_t) &= 16\left(\int_0^{t-T_{IPP}-T_{IPN}} \gamma(s)\beta(s)F_{AP}(s)ds\right) 1_{t \geq T_{IPP}+T_{IPN}} \\
&\quad + 4\left(\int_0^{t-T_{IPN}} (1-\gamma(s))\,\beta(s)F_{AP}(s)ds\right) 1_{t \geq T_{IPN}} \\
&\quad + \int_0^t (1-\beta(s))\,F_{AP}(s)ds.
\end{aligned}$$

In contrast to neurons, IPP and IPN do not accumulate along development. They are transit compartments, so that the instantaneous number $IPP(t)$ and $IPN(t)$ are far lower than the cumulated number of events 1 or events 2. More precisely, we have for all $t \geq 0$ from Equation (3)

$$IPP(t) = \sum_{k=1}^{Z_t^{AP}} 1_{Y_k=1, t-T_k<T_{IPP}} = Z_t^{(1)} - Z^{(1)}_{t-T_{IPP}} 1_{t \geq T_{IPP}}, \tag{17}$$

and similarly from Equation (4)

$$IPN(t) = 2\left(Z^{(1)}_{t-T_{IPP}} 1_{t\geq T_{IPP}} - Z^{(1)}_{t-T_{IPP}-T_{IPN}} 1_{t\geq T_{IPP}+T_{IPN}}\right) + \left(Z^{(2)}_t - Z^{(2)}_{t-T_{IPN}} 1_{t\geq T_{IPN}}\right). \quad (18)$$

From Equations (17) and (18), we can apply directly Lemma 1 to get the expectations.

Proposition 2. *For all $t \geq 0$,*

$$\begin{aligned}
\mathbb{E}[IPP(t)] &= \int_{\max(t-T_{IPP},0)}^{t} \gamma(s)\beta(s)F_{AP}(s)ds, \\
\mathbb{E}[IPN(t)] &= 2\int_{\max(t-T_{IPP}-T_{IPN},0)}^{\max(t-T_{IPP},0)} \gamma(s)\beta(s)F_{AP}(s)ds \\
&\quad + \int_{\max(t-T_{IPN},0)}^{t} (1-\gamma(s))\beta(s)F_{AP}(s)ds.
\end{aligned}$$

For the variances, we need an additional lemma.

Lemma 2. *For all $i \in \{1,2,3\}$, $t, s \geq 0$,*

$$\mathrm{Cov}(Z^{(i)}_t, Z^{(i)}_s) = \mathrm{Var}\left(Z^{(i)}_{\min(t,s)}\right).$$

Proof. Let $i \in \{1,2,3\}$, $t, s \geq 0$. The case when $s = t$ is straightforward. Without loss of generality, let us assume that $s < t$. We define the stochastic process $(\overline{Z}^{(i)}_r)_{r\geq 0}$ such that, for all $r \geq 0$,

$$\overline{Z}^{(i)}_r = \sum_{k=1}^{Z^{AP}_r} (1_{Y_k=i}1_{T_k\leq s}, 1_{Y_k=i}1_{T_k>s}) = \left(Z^{(i)}_{\min(r,s)}, \left(Z^{(i)}_r - Z^{(i)}_s\right)1_{r>s}\right).$$

One can see that $(\overline{Z}^{(i)}_r)_{r\geq 0}$ is a compound Poisson process with intensity F_{AP} and time-independent stochastic kernel L, such that, for all $r \geq 0$,

$$\begin{aligned}
L(r, dy) &= \mathbb{P}[Y_k = i \,|\, T_k = r]1_{r\leq s}\delta_{(1,0)}(dy) + \mathbb{P}[Y_k = i \,|\, T_k = r]1_{r>s}\delta_{(0,1)}(dy) \\
&\quad + (1 - \mathbb{P}[Y_k = i \,|\, T_k = r])\,\delta_{(0,0)}(dy).
\end{aligned}$$

We have $L(r, (\mathbb{R}\times\{0\}) \cup (\{0\}\times\mathbb{R})) = 1$ for any $r \geq 0$. Then, using Corollary 2 (as the kernel does not depend on time, $L = L_{t_1,t_2}$ for all t_1, $t_2 \geq 0$), we obtain that, for all $r \geq 0$, the random variables $Z^{(i)}_{\min(r,s)}$ and $\left(Z^{(i)}_r - Z^{(i)}_s\right)1_{r>s}$ are independent. In particular, for $r = t$, as $t > s$, the random variables $Z^{(i)}_s$ and $Z^{(i)}_t - Z^{(i)}_s$ are independent. Using now the independence between these variables, we have

$$\begin{aligned}
\mathbb{E}[Z^{(i)}_t Z^{(i)}_s] &= \mathbb{E}\left[\left(Z^{(i)}_t - Z^{(i)}_s\right)Z^{(i)}_s\right] + \mathbb{E}\left[\left(Z^{(i)}_s\right)^2\right] \\
&= \mathbb{E}\left[Z^{(i)}_t - Z^{(i)}_s\right]\mathbb{E}\left[Z^{(i)}_s\right] + \mathbb{E}\left[\left(Z^{(i)}_s\right)^2\right] \\
&= \mathbb{E}\left[Z^{(i)}_t\right]\mathbb{E}\left[Z^{(i)}_s\right] + \mathrm{Var}\left(Z^{(i)}_s\right).
\end{aligned}$$

Changing the side of $\mathbb{E}\left[Z^{(i)}_t\right]\mathbb{E}\left[Z^{(i)}_s\right]$ ends the proof. □

Using Lemma 2, we then get that for all $t \geq 0$,

$$\begin{aligned}\text{Var}\left(IPP(t)\right) &= \text{Var}(Z_t^{(1)}) + \text{Var}(Z_{t-T_{IPP}}^{(1)})1_{t\geq T_{IPP}} - 2\text{Var}(Z_{t-T_{IPP}}^{(1)})1_{t\geq T_{IPP}} \\ &= \text{Var}(Z_t^{(1)}) - \text{Var}(Z_{t-T_{IPP}}^{(1)})1_{t\geq T_{IPP}},\end{aligned}$$

and, using Corollary 2, and then Lemma 2,

$$\begin{aligned}\text{Var}(IPN(t)) &= 4\text{Var}(Z_{t-T_{IPP}}^{(1)}1_{t\geq T_{IPP}} - Z_{t-T_{IPP}-T_{IPN}}^{(1)}1_{t\geq T_{IPP}+T_{IPN}}) + \text{Var}(Z_t^{(2)} - Z_{t-T_{IPN}}^{(2)}1_{t\geq T_{IPN}}) \\ &= 4\Big(\text{Var}(Z_{t-T_{IPP}}^{(1)})1_{t\geq T_{IPP}} + \text{Var}(Z_{t-T_{IPP}-T_{IPN}}^{(1)})1_{t\geq T_{IPP}+T_{IPN}} \\ &- 2\text{Cov}(Z_{t-T_{IPP}}^{(1)}, Z_{t-T_{IPP}-T_{IPN}}^{(1)})1_{t\geq T_{IPP}+T_{IPN}}\Big) \\ &+ \Big(\text{Var}(Z_t^{(2)}) + \text{Var}(Z_{t-T_{IPN}}^{(2)})1_{t\geq T_{IPN}} - 2\text{Cov}(Z_t^{(2)}, Z_{t-T_{IPN}}^{(2)})1_{t\geq T_{IPN}}\Big) \\ &= 4\Big(\text{Var}(Z_{t-T_{IPP}}^{(1)})1_{t\geq T_{IPP}} - \text{Var}(Z_{t-T_{IPP}-T_{IPN}}^{(1)})1_{t\geq T_{IPP}+T_{IPN}}\Big) \\ &+ \Big(\text{Var}(Z_t^{(2)}) - \text{Var}(Z_{t-T_{IPN}}^{(2)})1_{t\geq T_{IPN}}\Big).\end{aligned}$$

Finally, applying Lemma 1 gives us the variances of $IPP(t)$ and $IPN(t)$ for all $t \geq 0$.

Proposition 3. *For all $t \geq 0$,*

$$\begin{aligned}\text{Var}(IPP(t)) = \mathbb{E}[IPP(t)] &= \int_{\max(t-T_{IPP},0)}^{t} \gamma(s)\beta(s)F_{AP}(s)ds, \\ \text{Var}(IPN(t)) &= 4\int_{\max(t-T_{IPP}-T_{IPN},0)}^{\max(t-T_{IPP},0)} \gamma(s)\beta(s)F_{AP}(s)ds \\ &+ \int_{\max(t-T_{IPN},0)}^{t} (1-\gamma(s))\beta(s)F_{AP}(s)ds.\end{aligned}$$

3.3 Application to neuron layering

We proceed in the same way as in the former subsection to derive the expectation and variance of the number of deep-layer neurons and upper-layer neurons (Equations (7)-(8)).
The final number of either deeper or upper layer neurons results from the combination of event 1, 2 or 3, with a second event associated with the "choice" of the layer type.
Let $t \geq 0$. For all $i \in \{1,2,3\}$, we denote $DL^{(i)}(t)$ the number of events associated with the choice of the deeper layers when an event i occurs at time t, which is also the final number of deeper-layer neurons at time t coming from events of type i, given that neurons neither divide nor die in the model. Formally, we have, for $i \in \{1,2,3\}$,

$$DL^{(i)}(t) = \sum_{k=1}^{Z^{AP}(t)} 1_{Y_k=i} B_k^{(i)}.$$

$(B_k^i)_{k\in\mathbb{N}^*, i\in\{1,2,3\}}$ is a sequence of independent variables conditionally to $(T_k)_{k\in\mathbb{N}^*}$, and independent of $(Y_k)_{k\in\mathbb{N}^*}$ conditionally to $(T_k)_{k\in\mathbb{N}^*}$, such that, for $k \in \mathbb{N}^*$,

$$
\begin{aligned}
B_k^{(1)}|T_k &= \text{Binom}(4, \Delta(T_k + T_{IPP} + T_{IPN})),\\
B_k^{(2)}|T_k &= \text{Binom}(2, \Delta(T_k + T_{IPN})),\\
B_k^{(3)}|T_k &= \text{Binom}(1, \Delta(T_k)).
\end{aligned}
$$

We can separate the contribution of each event 1, 2, 3 as follows

$$
DL(t) = DL^{(1)}(t - T_{IPP} - T_{IPN})1_{t \geq T_{IPP}+T_{IPN}} + DL^{(2)}(t - T_{IPN})1_{t \geq T_{IPN}} + DL^{(3)}(t).
$$

$(DL(s))_{s\geq 0}$ is thus a well-defined compound process. We can apply Corollary 1, and get the expectations and variances of $DL^{(1)}(t)$, $DL^{(2)}(t)$ and $DL^{(3)}(t)$. For instance, if we consider for all $s \geq 0$

$$
\begin{aligned}
L^{(1)}(s, dy) = &\sum_{i=1}^{4} \gamma(s)\beta(s)\mathbb{P}[\text{Binom}(4, \Delta(s + T_{IPP} + T_{IPN})) = i]\delta_i(dy)\\
&+ \left((1 - \gamma(s)\beta(s)) + \gamma(s)\beta(s)\mathbb{P}[\text{Binom}(4, \Delta(s + T_{IPP} + T_{IPN})) = 0]\right)\delta_0(dy),
\end{aligned}
$$

we have, using Corollary 1 and the fact that the first moment of a Binomial distribution $\text{Binom}(n, p)$ ($n \in \mathbb{N}$, $p \in [0, 1]$) is np,

$$
\begin{aligned}
\mathbb{E}[DL^{(1)}(t)] &= \int_0^t \left(\int_{\{0,1,2,3,4\}} yL^{(1)}(s, dy) \right) F_{AP}(s)ds\\
&= 4 \int_0^t \gamma(s)\beta(s)\Delta(s + T_{IPP} + T_{IPN})F_{AP}(s)ds.
\end{aligned}
$$

The same reasoning for $DL^{(2)}(t)$ and $DL^{(3)}(t)$ yields

$$
\begin{aligned}
\mathbb{E}[DL^{(2)}(t)] &= 2 \int_0^t (1 - \gamma(s))\, \beta(s)\Delta(s + T_{IPN})F_{AP}(s)ds,\\
\mathbb{E}[DL^{(3)}(t)] &= \int_0^t (1 - \beta(s))\, \Delta(s)F_{AP}(s)ds.
\end{aligned}
$$

For the variance, we have, using the fact that the second moment of a Binomial distribution $\text{Binom}(n, p)$ ($n \in \mathbb{N}$, $p \in [0, 1]$) is $n^2p^2 + np(1 - p) = n(n - 1)p^2 + np$,

$$
\begin{aligned}
\text{Var}(DL^{(1)}(t)) &= \int_0^t \left(\int_{\{0,1,2,3,4\}} y^2 L^{(1)}(s, dy) \right) F_{AP}(s)ds\\
&= 12 \int_0^t \gamma(s)\beta(s) \left(\Delta(s + T_{IPP} + T_{IPN})\right)^2 F_{AP}(s)ds\\
&+ 4 \int_0^t \gamma(s)\beta(s)\Delta(s + T_{IPP} + T_{IPN})F_{AP}(s)ds,
\end{aligned}
$$

and, with a similar reasoning,

$$
\begin{aligned}
\text{Var}(DL^{(2)}(t)) &= 2 \int_0^t (1 - \gamma(s))\, \beta(s) \left(\Delta^2 + \Delta\right)(s + T_{IPN})F_{AP}(s)ds,\\
\text{Var}(DL^{(3)}(t)) &= \int_0^t (1 - \beta(s))\, \Delta(s)F_{AP}(s)ds.
\end{aligned}
$$

From there, we get the expressions for $\mathbb{E}[DL(t)]$, $\mathrm{Var}(DL(t))$, $\mathbb{E}[UL(t)]$, and $\mathrm{Var}(UL(t))$, which are provided in the Appendix (Propositions 5 and 6 in Section 6.2).

3.4 Extension to stochastic cell cycle durations

The computation of the moments describing the progenitor dynamics in case of a stochastic cell cycle duration (Equations (10)-(11)-(12)) is based on the same reasoning as with a constant duration. The main difference arises from the fact that we have to handle compound Poisson processes with stochastic time-dependent kernels.
We begin by introducing the following notations to alleviate the computation.

Definition 4. *Let $\mu : \mathcal{B}(\mathbb{R}^+) \longrightarrow [0,1]$ a probability measure, and a measurable function $f : \mathbb{R}^+ \longrightarrow \mathbb{R}$. Then we define $*$ the operation such that for all $t \geq 0$*

$$(f * \mu)(t) = \int_0^t f(t-s)d\mu(s).$$

Definition 5. *For any measure μ, we can consider the cumulative distribution function, and the survival function associated with μ, defined for all $t \geq 0$ as*

$$G(t) = \mu([0,t]) = \int_0^t d\mu(s),$$
$$\overline{G}(t) = 1 - G(t).$$

Definition 6. *Let $\mu : \mathcal{B}(\mathbb{R}^+) \longrightarrow [0,1]$ a probability measure, $f : \mathbb{R}^+ \longrightarrow \mathbb{R}$ a measurable function, and $0 \leq a \leq b$ two real numbers. Then we use the notation*

$$\mu(f([a,b])) = \int_0^{b-a} f(x+a)dx.$$

Using Definition 5, we denote μ_{IPP} the probability measure of the cell cycle duration of IPPs, G_{IPP} and $\overline{G}_{IPP}$ its associated cumulative distribution and survival function. We do the same for the cell cycle duration of IPNs. Let $t \geq 0$. For each cell type, for all $k \in [\![1, Z_t^{AP}]\!]$, we will introduce the stochastic processes $(A_s^{(k)})_{s\geq 0}$, subject to the laws of IPP and IPN cell cycle durations, whose conditional law with respect to T_k informs on the contribution of each pathway (event 1, 2 or 3) in the current cell numbers $IPP(t)$, $IPN(t)$ and $N(t)$. Then, what we need is to obtain the kernels of the $(A_s^{(k)})_{s\geq 0}$ processes, hence of the underlying compound Poisson process. Once this step is performed, we can apply Corollary 1 with the proper stochastic kernel to obtain the expectations (see Equation (19)) and variances (see Equation (20)) of the cell type numbers enunciated in Proposition 4.

Proposition 4. *For all $t \geq 0$, we have*

$$\begin{aligned}
\mathbb{E}\left[IPP(t)\right] &= \int_0^t \gamma(s)\beta(s)\overline{G}_{IPP}(t-s)F_{AP}(s)ds, \\
\mathbb{E}[IPN(t)] &= 2\int_0^t \gamma(s)\beta(s)\left(\overline{G}_{IPN} * \mu_{IPP}\right)(t-s)F_{AP}(s)ds \\
&+ \int_0^t (1-\gamma(s))\,\beta(s)\overline{G}_{IPN}(t-s)F_{AP}(s)ds, \\
\mathbb{E}[N(t)] &= 4\int_0^t \gamma(s)\beta(s)\left(G_{IPN} * \mu_{IPP}\right)(t-s)F_{AP}(s)ds \\
&+ 2\int_0^t (1-\gamma(s))\,\beta(s)G_{IPN}(t-s)F_{AP}(s)ds \\
&+ \int_0^t (1-\beta(s))\,F_{AP}(s)ds,
\end{aligned} \tag{19}$$

and

$$\begin{aligned}
\mathrm{Var}\left(IPP(t)\right) &= \int_0^t \gamma(s)\beta(s)\overline{G}_{IPP}(t-s)F_{AP}(s)ds, \\
\mathrm{Var}(IPN(t)) &= 2\int_0^t \gamma(s)\beta(s)\left(\overline{G}^2_{IPN} * \mu_{IPP}\right)(t-s)F_{AP}(s)ds, \\
&+ 2\int_0^t \gamma(s)\beta(s)\left(\overline{G}_{IPN} * \mu_{IPP}\right)(t-s)F_{AP}(s)ds \\
&+ \int_0^t (1-\gamma(s))\,\beta(s)\overline{G}_{IPN}(t-s)F_{AP}(s)ds, \\
\mathrm{Var}(N(t)) &= 8\int_0^t \gamma(s)\beta(s)\left(G^2_{IPN} * \mu_{IPP}\right)(t-s)F_{AP}(s)ds \\
&+ 8\int_0^t \gamma(s)\beta(s)\left(G_{IPN} * \mu_{IPP}\right)(t-s)F_{AP}(s)ds \\
&+ 4\int_0^t (1-\gamma(s))\,\beta(s)G_{IPN}(t-s)F_{AP}(s)ds \\
&+ \int_0^t (1-\beta(s))\,F_{AP}(s)ds.
\end{aligned} \tag{20}$$

Proof. Let $t \geq 0$. Let us start with $IPP(t)$. We have

$$IPP(t) = \sum_{k=1}^{Z_t^{AP}} A_t^{(k,1)},$$

where for any $k \in \mathbb{N}^*$

$$A_t^{(k,1)} = 1_{Y_k=1}1_{T_k+S_k>t},$$

and $(S_k)_{k\in\mathbb{N}^*}$ are stochastic variables whose laws are associated with probability measure μ_{IPP}. To apply Corollary 1, we compute the associated stochastic kernel from the distribution of $A_t^{(k,1)}$ conditionally to T_k. We have for all $k \in \mathbb{N}^*$

$$\begin{aligned}\mathbb{P}[A_t^{(k,1)} = 1 \,|\, T_k] &= \mathbb{P}[Y_k = 1, S_k > t - T_k \,|\, T_k] \\ &= \mathbb{P}[Y_k = 1 \,|\, T_k]\mathbb{P}[S_k > t - T_k \,|\, T_k] \\ &= \gamma(T_k)\beta(T_k)\overline{G}_{IPP}(t - T_k),\end{aligned}$$

and conversely $\mathbb{P}[A_t^{(k,1)} = 0|T_k] = 1 - \gamma(T_k)\beta(T_k)\overline{G}_{IPP}(t - T_k)$. Then, the direct application of Corollary 1 gives $\mathbb{E}[IPP(t)]$ and $\mathrm{Var}[IPP(t)]$ in Proposition 4.
In the case of $IPN(t)$, we have

$$IPN(t) = \sum_{k=1}^{Z_t^{AP}} A_t^{(k,2)},$$

where, for any $k \in \mathbb{N}^*$,

$$A_t^{(k,2)} = 1_{Y_k=1}\left(1_{T_k+S_k+R_k^{(1,1)}>t\geq T_k+S_k} + 1_{T_k+S_k+R_k^{(1,2)}>t\geq T_k+S_k}\right) + 1_{Y_k=2}1_{T_k+R_k^{(2)}>t}.$$

Again, we compute the stochastic kernel in the same way as for $IPP(t)$:

$$\begin{aligned}\mathbb{P}[A_t^{(k,2)} = 2 \,|\, T_k] &= \mathbb{P}[1_{Y_k=1} = 1, 1_{T_k+S_k+R_k^{(1,1)}>t\geq T_k+S_k} = 1, 1_{T_k+S_k+R_k^{(1,2)}>t\geq T_k+S_k} = 1 \,|\, T_k] \\ &= \mathbb{P}\left[Y_k = 1 \,|\, T_k\right]\mathbb{P}\left[S_k + R_k^{(1,1)} > t - T_k \geq S_k,\, S_k + R_k^{(1,2)} > t - T_k \geq S_k \,|\, T_k\right] \\ &= \mathbb{P}\left[Y_k = 1 \,|\, T_k\right]\left(\int_{0\leq s\leq t-T_k<s+r_1 \text{ and } t-T_k<s+r_2} \left(d\mu_{IPP} \times d\mu_{IPN} \times d\mu_{IPN}\right)(s, r_1, r_2)\right).\end{aligned}$$

We can further develop $(d\mu_{IPP} \times d\mu_{IPN} \times d\mu_{IPN})$, and get

$$\begin{aligned}\mathbb{P}[A_t^{(k,2)} = 2 \,|\, T_k] &= \mathbb{P}\left[Y_k = 1 \,|\, T_k\right]\left(\int_0^{t-T_k} \left(\mu_{IPN} \times \mu_{IPN}\right)\left(]t - T_k - s, +\infty[^2\right) d\mu_{IPP}(s)\right) \\ &= \mathbb{P}\left[Y_k = 1 \,|\, T_k\right]\left(\int_0^{t-T_k} \left(\mu_{IPN}\left(]t - T_k - s, +\infty[\right)\right)^2 d\mu_{IPP}(s)\right) \\ &= \gamma(T_k)\beta(T_k)\left(\int_0^{t-T_k} \left(\overline{G}_{IPN}\left(t - T_k - s\right)\right)^2 d\mu_{IPP}(s)\right) \\ &= \gamma(T_k)\beta(T_k)\left(\overline{G}_{IPN}^2 * \mu_{IPP}\right)(t - T_k).\end{aligned}$$

On the other hand, by symmetry, we have

$$\begin{aligned}\mathbb{P}[A_t^{(k,2)} = 1 \,|\, T_k] &= \mathbb{P}[Y_k = 1, A_t^{(k,2)} = 1 \,|\, T_k] + \mathbb{P}[Y_k = 2, A_t^{(k,2)} = 1 \,|\, T_k] \\ &= 2\mathbb{P}\left[Y_k = 1 \,|\, T_k\right]\mathbb{P}\left[1_{T_k+S_k+R_k^{(1,1)}>t\geq T_k+S_k} = 1, 1_{T_k+S_k+R_k^{(1,2)}>t\geq T_k+S_k} = 0 \,|\, T_k\right] \\ &+ \mathbb{P}[Y_k = 2 \,|\, T_k]\mathbb{P}[R_k^{(2)} > t - T_k \,|\, T_k] \\ &= 2\mathbb{P}\left[Y_k = 1 \,|\, T_k\right]\mathbb{P}\left[S_k + R_k^{(1,1)} > t - T_k \geq S_k,\, S_k + R_k^{(1,2)} \leq t - T_k \,|\, T_k\right] \\ &+ \left(1 - \gamma(T_k)\right)\beta(T_k)\overline{G}_{IPN}(t - T_k).\end{aligned}$$

Given that

$$\begin{aligned}
&\mathbb{P}\left[S_k + R_k^{(1,1)} > t - T_k \geq S_k,\, S_k + R_k^{(1,2)} \leq t - T_k \,|\, T_k\right] \\
&= \int_{0\leq s\leq t-T_k<s+r_1 \text{ and } t-T_k\geq s+r_2} \left(d\mu_{IPP} \times d\mu_{IPN} \times d\mu_{IPN}\right)(s, r_1, r_2) \\
&= \int_0^{t-T_k} \left(\mu_{IPN} \times \mu_{IPN}\right)(]t - T_k - s, +\infty[\times[0, t - T_k - s])d\mu_{IPP}(s) \\
&= \int_0^{t-T_k} \overline{G}_{IPN}(t - T_k - s)G_{IPN}(t - T_k - s)d\mu_{IPP}(s) = \left(\overline{G}_{IPN}G_{IPN} * \mu_{IPP}\right)(t - T_k),
\end{aligned}$$

we get

$$\begin{aligned}
\mathbb{P}[A_t^{(k,2)} = 1 \,|\, T_k] = 2\gamma(T_k)\beta(T_k)\left(\overline{G}_{IPN}G_{IPN} * \mu_{IPP}\right)(t - T_k) \\
+ (1 - \gamma(T_k))\,\beta(T_k)\overline{G}_{IPN}(t - T_k).
\end{aligned}$$

If we denote $\left(L_s^{(2)}\right)_{s\geq 0}$, the stochastic kernel associated with $\left(A_s^{(l,2)}\right)_{s\geq 0, l\in\mathbb{N}^*}$, we finally have, for all $s \geq 0$, using the equality $\overline{G}_{IPN}^2 + \overline{G}_{IPN}G_{IPN} = \overline{G}_{IPN}$,

$$\begin{aligned}
\int_{\mathbb{R}} yL_t^{(2)}(s, dy) &= 2.\mathbb{P}[A_t^{(k,2)} = 2 \,|\, T_k = s] + 1.\mathbb{P}[A_t^{(k,2)} = 1 \,|\, T_k = s] \\
&= 2\gamma(s)\beta(s)\left(\overline{G}_{IPN}^2 * \mu_{IPP}\right)(t - s) \\
&+ 2\gamma(s)\beta(s)\left(\overline{G}_{IPN}G_{IPN} * \mu_{IPP}\right)(t - s) \\
&+ (1 - \gamma(s))\,\beta(s)\overline{G}_{IPN}(t - s) \\
&= 2\gamma(s)\beta(s)\left(\overline{G}_{IPN} * \mu_{IPP}\right)(t - s) + (1 - \gamma(s))\,\beta(s)\overline{G}_{IPN}(t - s),
\end{aligned}$$

and

$$\begin{aligned}
\int_{\mathbb{R}} y^2L_t^{(2)}(s, dy) &= 4.\mathbb{P}[A_t^{(k,2)} = 2 \,|\, T_k = s] + 1.\mathbb{P}[A_t^{(k,2)} = 1 \,|\, T_k = s] \\
&= 2\gamma(s)\beta(s)\left(\overline{G}_{IPN}^2 * \mu_{IPP}\right)(t - s) \\
&+ 2\gamma(s)\beta(s)\left(\overline{G}_{IPN} * \mu_{IPP}\right)(t - s) \\
&+ (1 - \gamma(s))\,\beta(s)\overline{G}_{IPN}(t - s).
\end{aligned}$$

We finally apply Corollary 1 to obtain $\mathbb{E}[IPNt)]$ and $\mathrm{Var}[IPN(t)]$ in Proposition 4.
The computation for $N(t)$ is close to that developed for $IPN(t)$. First, we have

$$N(t) = \sum_{k=1}^{Z_t^{AP}} A_t^{(k,3)},$$

where for all $k \in \mathbb{N}^*$

$$A_t^{(k,3)} = 1_{Y_k=1}\left(21_{T_k+S_k+R_k^{(1,1)}\leq t} + 21_{T_k+S_k+R_k^{(1,2)}\leq t}\right) + 21_{Y_k=2}1_{T_k+R_k^{(2)}\leq t} + 1_{Y_k=3}.$$

As in the case of $IPN(t)$, we compute separately the probability of $A_t^{(k,3)}$ given T_k. First, we easily have

$$\mathbb{P}[A_t^{(k,3)} = 1 \,|\, T_k] = \mathbb{P}[Y_k = 3 \,|\, T_k] = 1 - \beta(T_k).$$

Second, we have

$$\begin{aligned}
\mathbb{P}[A_t^{(k,3)} = 4 \,|\, T_k] &= \mathbb{P}[Y_k = 1 \,|\, T_k]\mathbb{P}[T_k + S_k + R_k^{(1,1)} \leq t,\, T_k + S_k + R_k^{(1,2)} \leq t \,|\, T_k] \\
&= \mathbb{P}[Y_k = 1 \,|\, T_k] \left(\int_{s+r_1 \leq t-T_k \text{ and } s+r_2 \leq t-T_k} (d\mu_{IPP} \times d\mu_{IPN} \times d\mu_{IPN})(s, r_1, r_2) \right) \\
&= \mathbb{P}[Y_k = 1 \,|\, T_k] \left(\int_0^{t-T_k} G_{IPN}^2(t - T_k - s) d\mu_{IPP}(s) \right) \\
&= \gamma(T_k)\beta(T_k) \left(G_{IPN}^2 * \mu_{IPP} \right)(t - T_k).
\end{aligned}$$

Finally, we have, by symmetry

$$\begin{aligned}
\mathbb{P}[A_t^{(k,3)} = 2 \,|\, T_k] &= \mathbb{P}[A_t^{(k,3)} = 2, Y_k = 1 \,|\, T_k] + \mathbb{P}[A_t^{(k,3)} = 2, Y_k = 2 \,|\, T_k] \\
&= 2\mathbb{P}[T_k + S_k + R_k^{(1,1)} \leq t, T_k + S_k + R_k^{(1,2)} > t, Y_k = 1 \,|\, T_k] \\
&\quad + \mathbb{P}[T_k + R_k^{(2)} \leq t, Y_k = 2 \,|\, T_k].
\end{aligned}$$

Thanks to the independence property, and recalling that, conditionally to T_k, $R_k^{(2)}$ is distributed according to probability measure G_{IPN}, we get

$$\begin{aligned}
\mathbb{P}[A_t^{(k,3)} = 2 \,|\, T_k] &= 2\mathbb{P}[T_k + S_k + R_k^{(1,1)} > t, T_k + S_k + R_k^{(1,2)} \leq t \,|\, T_k]\mathbb{P}[Y_k = 1 \,|\, T_k] \\
&\quad + \mathbb{P}[T_k + R_k^{(2)} \leq t \,|\, T_k]\mathbb{P}[Y_k = 2 \,|\, T_k]. \\
&= 2\mathbb{P}[T_k + S_k + R_k^{(1,1)} > t, T_k + S_k + R_k^{(1,2)} \leq t \,|\, T_k]\gamma(T_k)\beta(T_k) \\
&\quad + G_{IPN}(t - T_k)\left(1 - \gamma(T_k)\right)\beta(T_k).
\end{aligned}$$

Using the following relation (retrieved from the similar computation in the case of $IPN(t)$)

$$\mathbb{P}[T_k + S_k + R_k^{(1,1)} > t, T_k + S_k + R_k^{(1,2)} \leq t \,|\, T_k] = \left(\overline{G}_{IPN} G_{IPN} * \mu_{IPP}\right)(t - T_k),$$

we obtain

$$\mathbb{P}[A_t^{(k,3)} = 2 \,|\, T_k] = 2\left(\overline{G}_{IPN} G_{IPN} * \mu_{IPP}\right)(t - T_k)\gamma(T_k)\beta(T_k) + G_{IPN}(t - T_k)\left(1 - \gamma(T_k)\right)\beta(T_k).$$

Then, if we denote $\left(L_s^{(3)}\right)_{s \geq 0}$, the stochastic kernel associated with $\left(A_s^{(l,3)}\right)_{s \geq 0, l \in \mathbb{N}^*}$, and use the equality $G_{IPN}^2 + G_{IPN}\overline{G}_{IPN} = G_{IPN}$, we obtain for all $s \geq 0$

$$\begin{aligned}
\int_{\mathbb{R}} y L_t^{(3)}(s, dy) &= 4.\mathbb{P}[A_t^{(k,3)} = 4 \,|\, T_k = s] + 2.\mathbb{P}[A_t^{(k,3)} = 2 \,|\, T_k = s] + 1.\mathbb{P}[A_t^{(k,3)} = 1 \,|\, T_k = s] \\
&= 4\gamma(s)\beta(s)\left(G_{IPN} * \mu_{IPP}\right)(t - s) \\
&\quad + 2\left(1 - \gamma(s)\right)\beta(s) G_{IPN}(t - s) \\
&\quad + 1 - \beta(s),
\end{aligned}$$

and for the variance

$$\begin{aligned}\int_{\mathbb{R}} y^2 L_t^{(3)}(s,dy) &= 16.\mathbb{P}[A_t^{(k,3)} = 4 \,|\, T_k = s] + 4.\mathbb{P}[A_t^{(k,3)} = 2 \,|\, T_k = s] + 1.\mathbb{P}[A_t^{(k,3)} = 1 | T_k = s] \\ &= 8\gamma(s)\beta(s)\left(G_{IPN}^2 * \mu_{IPP}\right)(t-s) \\ &+ 8\gamma(s)\beta(s)\left(G_{IPN} * \mu_{IPP}\right)(t-s) \\ &+ 4\left(1-\gamma(s)\right)\beta(s) G_{IPN}(t-s) \\ &+ 1 - \beta(s).\end{aligned}$$

Applying Corollary 1 finally gives the expressions for $\mathbb{E}[N(t)]$ and $\mathrm{Var}(N(t))$ in Proposition 4. □

Using the ideas introduced in Section 3.3, we can in the save may derive the expressions for the expectations and variances of the deeper- and upper- neurons (Equations (13)-(14)). We detail the computations in the Appendix (see Section 6.3).

4 Numerical illustrations and experimental data fitting

In this section, we provide a panel of numerical results illustrating our theoretical analysis. We begin with presenting the algorithm implemented to perform exact simulations with time-varying intensities. We then perform a thorough comparison between the original deterministic model and the newly designed stochastic model. We discuss the impact of choosing a non-constant, stochastically distributed duration of the cell cycle on the dynamics of intermediate progenitors. Then we compare all model outputs to experimental data, using a yet unexploited dataset to fit the number of deeper- and upper-layer neurons.

4.1 Exact numerical simulation

4.1.1 Overview of the whole simulation steps

The pseudo-code corresponding to a whole simulation is described in Algorithm 1, for the most extended version of the model, including neuron layering and stochastic cell cycles. The core algorithm steps are:

1. Simulate the next update time ($t + t_{event}$) from an Exponential law;
2. Select the division type (event 1, 2 or 3), through classical acceptance-reject from the realization of a stochastic variable following a Uniform distribution;
3. In the case of stochastic cell cycle durations, compute the value of T_{IPP} and/or T_{IPN} through the inverse of the distribution functions G_{IPP}^{-1} and/or G_{IPN}^{-1} applied to the realization a Uniform distribution;
4. Select the neuron layers through classical acceptance-reject from direct drawing from a Binomial law;
5. Update the cell numbers of each cell type (IPP, IPN, N, DL, UL).

Algorithm 1 Exact simulation with time-varying intensities and stochastic cell cycle durations.

times $\leftarrow$ arange(start, end, step)
IPP $\leftarrow$ zeros(len(times))
IPN $\leftarrow$ zeros(len(times))
N $\leftarrow$ zeros(len(times))
DL $\leftarrow$ zeros(len(times))
UL $\leftarrow$ zeros(len(times))
$t \leftarrow t_{\text{start}}$
while $t < t_{\text{end}}$ **do**
    $t_{\text{event}} \leftarrow \mathcal{E}(\overline{F})$
    if $t + t_{\text{event}} > t_{\text{end}}$ **then**
        t $\leftarrow t_{\text{end}}$
    else
        $t \leftarrow t + t_{\text{event}}$
        whichdiv $\leftarrow U([0,1])\overline{F}$
        if whichdiv $\leq \gamma(t)\beta(t)F_{AP}(t)$ **then**
            $T_{IPP} = G_{IPP}^{-1}(U([0,1]))$
            IPP$[t : t + T_{IPP}]$ += 1
            for $i = 1, 2$ **do**
                $T_{IPN}^{(i)} = G_{IPN}^{-1}(U([0,1]))$
                IPN$[t + T_{IPP} : t + T_{IPP} + T_{IPN}^{(i)}]$ += 1
                newDL = Binom $\left(2, \Delta(t + T_{IPP} + T_{IPN}^{(i)})\right)$
                DL$[t + T_{IPP} + T_{IPN}^{(i)} : \text{end}]$ += newDL
                UL$[t + T_{IPP} + T_{IPN}^{(i)} : \text{end}]$ += (2 − newDL)
        else if $\gamma(t)\beta(t)F_{AP}(t) \leq$ whichdiv $\leq \beta(t)F_{AP}(t)$ **then**
            $T_{IPN} = G_{IPN}^{-1}(U([0,1]))$
            IPN$[t : t + T_{IPN}]$ += 1
            newDL = Binom $(2, \Delta(t + T_{IPN}))$
            DL$[t + T_{IPN} : \text{end}]$ += newDL
            UL$[t + T_{IPN} : \text{end}]$ += (2 − newDL)
            N$[t + T_{IPN} : \text{end}]$ += 2
        else if $\beta(t)F_{AP}(t) \leq$ whichdiv $\leq F_{AP}(t)$ **then**
            newDL = Binom $(1, \Delta(t))$
            DL$[t : \text{end}]$ += newDL
            UL$[t : \text{end}]$ += (1 − newDL)
            N$[t : \text{end}]$ += 1
        else
            Nothing (update R_t)
return times, IPP, IPN, N, DL, UL

4.1.2 Accounting for time-varying intensities

In the model, new events occur at rate $F_{AP}(t)$, which depends explicitly on time. To perform exact simulations of the stochastic process $(Z_t^{AP})_{t\geq 0}$, we have to account for this time-dependency

and update the value of F_{AP} between two subsequent events. We apply the "Extrande" strategy introduced in [30], which is valid for bounded rates. Namely : there exists $\overline{F} \in \mathbb{R}^+$ so that, for all $t \geq 0$, $|F_{AP}(t)| \leq \overline{F}$.
We introduce $(R_t)_{t\geq 0}$, the Poisson process with intensity $\overline{F} - F_{AP}(t)$, and define the new process $(Z_t)_{t\geq 0}$, such that for all $t \geq 0$, $Z_t = (Z_t^{AP}, R_t)$. $(Z_t)_{t\geq 0}$ is updated with intensity $F_{AP} + \left(\overline{F} - F_{AP}\right) = \overline{F}$ (hence the minimum rate of the Exponential laws associated with $(Z_t^{AP})_{t\geq 0}$ and $(R_t)_{t\geq 0}$).
The underlying idea is to consider additional rejection cases which become active when the value of rate F_{AP} cannot be assumed to be unchanged since the last event. $(R_t)_{t\geq 0}$ is used as an auxiliary process, and $(Z_t^{AP})_{t\geq 0}$ is obtained from the first three coordinates of $(Z_t)_{t\geq 0}$.

Accordingly, in Algorithm 1, at each iteration, the very first step consists in simulating the next update time of $(Z_t)_{\geq 0}$ from the Exponential law $\mathcal{E}(\overline{F})$ (rather than $\mathcal{E}(F_{AP}(t))$ where $t \geq 0$), and the condition loop includes another step, when all cell events are rejected. In this case nothing happens from the cell dynamics viewpoint, process $(R_t)_{t\geq 0}$ is just updated.

4.2 Comparison between the stochastic and deterministic models

4.2.1 Constant cell cycle durations

The dynamics of IPP, IPN and neuron populations are computed from the rate functions and optimal parameter values provided in [23] for both wild-type and mutant mice.
The shape of function $F_{AP}(t)$ in Equation (21) meets the requirement that the outflow from APs is restricted to a specific developmental time window, with the onset of neurogenesis on one side and the offset through gliogenesis on the other side (see Figure 7 in Section 6.4). Function $\gamma(t)$ in Equation (22) is an increasing sigmoid function. For all $t \geq 0$,

$$F_{AP}(t) = K_{AP} \frac{e^{s_+(t-t_+)}}{\left(1+e^{s_+(t-t_+)}\right)\left(1+e^{s_-(t-t_-)}\right)}, \tag{21}$$

$$\gamma(t) = \gamma_1 + \frac{\gamma_0 - \gamma_1}{\left(1+e^{s_\gamma(t-t_\gamma)}\right)}. \tag{22}$$

The parameter values, as well as the durations of the IPP and IPN cell cycles, are gathered in Table 2. Direct neurogenesis appeared to be negligible, so that we do not use $\beta(t)$ in this section (in other words $\beta(t) = 1$).

Parameter	K_{AP}	s_+	t_+	s_-	t_-	γ_0	γ_1	s_γ	t_γ	T_{IPP}	T_{IPN}
Unit	cell.d^{-1}	d^{-1}	d	d^{-1}	d	-	-	d^{-1}	d	d	d
Wild-Type	213.6	3.17	11.91	3.12	17.14	0.28	0.46	10	14.32	1.225	1.091
Mutant	850.08	1.51	14.10	1.07	14.87	0	0.48	10	13.90		

Table 2: Parameter values for progenitor dynamics in wild-type and mutant mice.

To illustrate our theoretical results, we performed a series of comparisons, between individual trajectories of the stochastic model, the expectations of cell numbers and the outputs of the deterministic

model (Figure 2). The expectations are computed according to the formulas provided in Propositions 1 and 2 using a quadrature rule for integrals. In the case of constant cell cycle durations, the expressions of the expectations correspond exactly to the integral solutions of the deterministic model, which can be solved by the method of characteristics. Hence, the consistency observed in Figure 2 between the expectations of the stochastic model and the solutions of the deterministic model is expected. In addition, the empirical mean appears to be an accurate estimate of the expectation, even with a relatively low number (500) of trajectories. Computing the expectation is numerically costly compared to computing the empirical mean, so that we will make use of the empirical mean in several instances in the sequel.

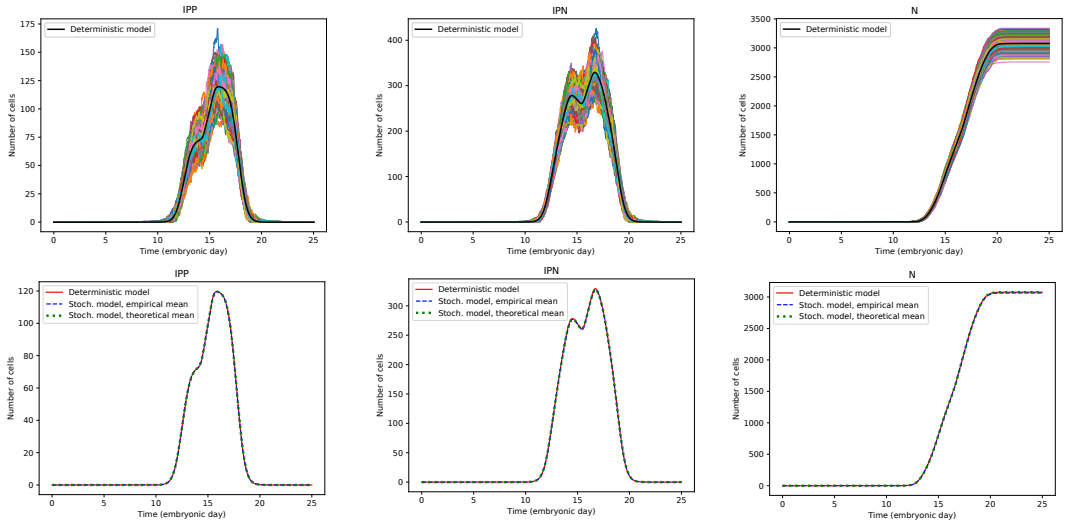

Figure 2: Comparison between the stochastic and deterministic models. *Upper panels: Comparison between 500 stochastic trajectories and the deterministic model outputs (superimposed black solid lines). Lower panels: Comparison between the computed expectations of the stochastic model (green dotted lines), the empirical means (blue dashed lines) and the deterministic model (red solid lines). Left panels: $IPP(t)$, middle panels: $IPN(t)$, right panels: $N(t)$.*

4.2.2 Stochastic cell cycle durations

To explore the effect of a non-constant stochastic cell cycle duration, we drew stochastic variables from three different distributions: the Exponential law, the Gamma law, and a customized formulation of the Beta(-symmetric) law, denoted by $\beta^*(c,\alpha)$ where $c,\alpha>0$ are two positive parameters. Then, the probability density function associated with $\beta^*(c,\alpha)$ is for all $x \geq 0$

$$g_{\beta^*(c,\alpha)}(x) = \frac{\left(\frac{x}{c}\right)^\alpha \left(1-\frac{x}{c}\right)^\alpha}{c\int_0^1 y^\alpha (1-y)^\alpha dy} 1_{[0,c]}(x).$$

Remark 5. *We notice that if $X \sim \beta^*(c,\alpha)$ where $c,\alpha>0$, then $X \overset{(law)}{=} cY$ where $Y \sim \beta(\alpha,\alpha)$ (β is the usual Beta distribution).*

In all cases, the parameters of the law were chosen in such a way that the expectation corresponds to the constant values of T_{IPP} and T_{IPN} (Table 2).
In the Gamma and (symmetric-)Beta cases, we also fix the parameters to set the variability to around 20 to 30% of the mean value, namely $\sigma^2_{T_{IPP}} = 0.4$, and $\sigma^2_{T_{IPN}} = 0.35$. We recall the relation between the parameters, expectation and variance:

- $\Gamma(k, \theta)$ law, with $(k, \theta) \in (\mathbb{R}^+)^2$: $k = \dfrac{\mathbb{E}[X]^2}{\mathrm{Var}(X)}$, $\theta = \dfrac{\mathbb{E}[X]}{\mathrm{Var}(X)}$,
- $\beta^*(c, \alpha)$ law, with $(c, \alpha) \in (\mathbb{R}^+_*)^2$: $c = 2\mathbb{E}[X]$, $\alpha = \dfrac{1}{2}\left(\dfrac{\mathbb{E}[X]^2}{\mathrm{Var}(X)} - 1\right)$.

An instance of simulation with a Gamma law is shown on Figure 3.

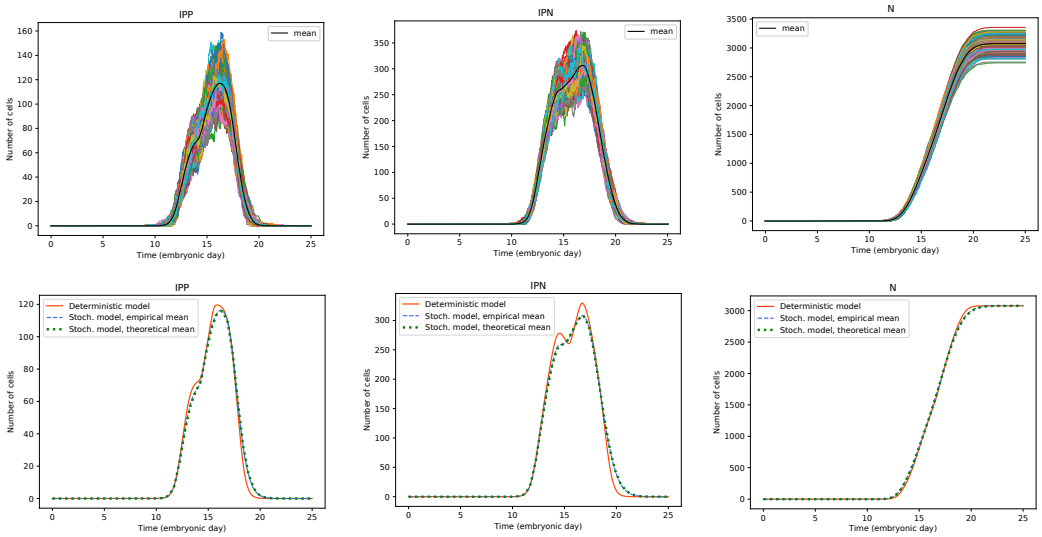

Figure 3: Comparison between the stochastic and deterministic models in case of stochastically-distributed durations of cell cycles. *The durations were drawn according to a Gamma law. Upper panels : The black curves superimposed over 500 stochastic trajectories correspond to the empirical means. Lower panels: comparison between the computed expectations of the stochastic model (green dotted lines), the empirical means (blue dashed lines) and the deterministic model outputs (red solid lines). Left panels: IPP(t), middle panels: IPN(t), right panels: N(t).*

We can observe a clear difference between the stochastic mean and the deterministic output. Such a difference is also observed with the other choices of distribution (see Figure 4). Introducing variability in the cell cycle duration blurs the bimodal pattern observed in $IPP(t)$, and even more in $IPN(t)$. In all cases, the IPN pattern results from the combination of direct IPN production (from AP through event 2) and indirect production (from IPP through event 1), whose balance is ruled by $\gamma(t)$. In the case of deterministic cell cycle durations, the IPN pattern is further shaped by the constant transit time, T_{IPP}, along the IPP state. Before the switch in $\gamma(t)$, occurring close to E14 (see Figure 7), the number of IPP was about to plateauing, since a balance between almost constant inflow from APs and the same outflow into IPN (delayed from T_{IPP}) was being established.

The increase in the AP to IPP inflow, due to the jump in $\gamma(t)$, then restores an increasing slope up to the IPP peak value. Yet the impact on indirect IPN production can be seen only one cell cycle later, so that, in a first time, it does not compensate for the cumulative effect of generating the earliest neurons and dropping $(1-\gamma(t))$ direct inflow from AP, hence the valley observed around E15. Afterwards, the "arrival" of IPP generated after the switching time restarts the increase in the IPN number, all the more since one IPP cell gives birth to 2 IPN cells, and the AP-derived IPNs plateau before decreasing again, hence the higher second bump. In the case of stochastic cell cycle durations, the arrival time of IPP cells born after the switch in $\gamma(t)$ is smoothed, as the synchronization arising from the constant T_{IPP} delay disappears, and only a more or less shouldering (according to the chosen variance in the duration distribution) can be observed on the total IPN curve.

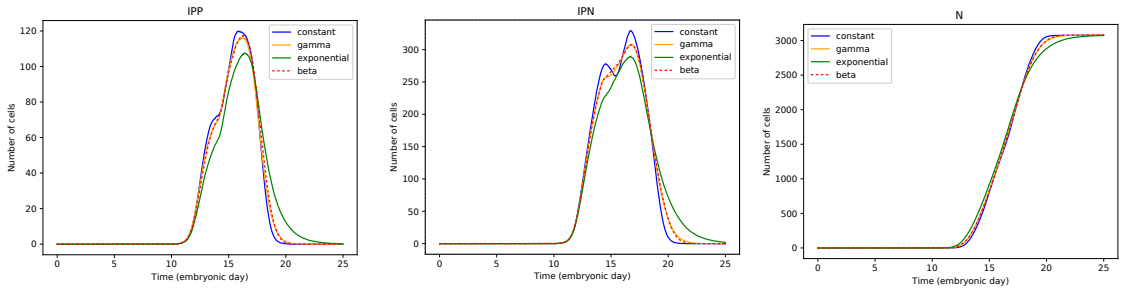

Figure 4: Expectations of each cell type for different cell cycle distributions. *On each panel, the expectation is assessed by the empirical mean computed over 500 stochastic trajectories, and the choice of the distribution is color-encoded (red lines : Beta distribution. green lines : Exponential distribution, yellow lines : Gamma distribution). For sake of comparison, the deterministic outputs are also displayed (blue lines). Left panels: IPP(t), middle panels: IPN(t), right panels: N(t).*

4.3 Data-fitting

4.3.1 Experimental data

In this section, we used data corresponding to both wild-type mice and mice mutant for *Ftm/Rpgrip1l*, a gene involved in the formation of a cell organelle, the primary cilium. *Ftm/Rpgrip1l*$^{-/-}$ mice suffer from severe brain anomalies [3], as encountered in some human ciliopathies.
The dataset consists of the cell numbers for each progenitor type (AP, IPP or IPN) or neuron type (UL or DL). The raw data are provided as a supplemental file in [23].
The dataset covers the embryonic time window from embryonic age 12.5 to 18.5, on a daily basis. Classification of the cell types relied on both the anatomical location (ventricular zone, subventricular zone or cortical plate, separating respectively APs from IPs and IPs from neurons) and specific staining (see Table 3).

4.3.2 Fitting of progenitor dynamics

For progenitor dynamics, we use the same parameter values as in Section 4.2 in the wild-type case, and the mutant specific values in Table 2. The resulting changes in cell numbers are illustrated on

Neural type	Staining
AP	Pax6+Tbr2-
IPP	Pax6+Tbr2+
IPN	Tbr2+Ctip2-
UL	Satb2+
DL	Ctip2+ Satb2-

Table 3: Molecular markers used for progenitor and neuron classification.

Figure 5, and the corresponding time changes in functions F_{AP} and γ are shown in the Appendix (Figure 7).

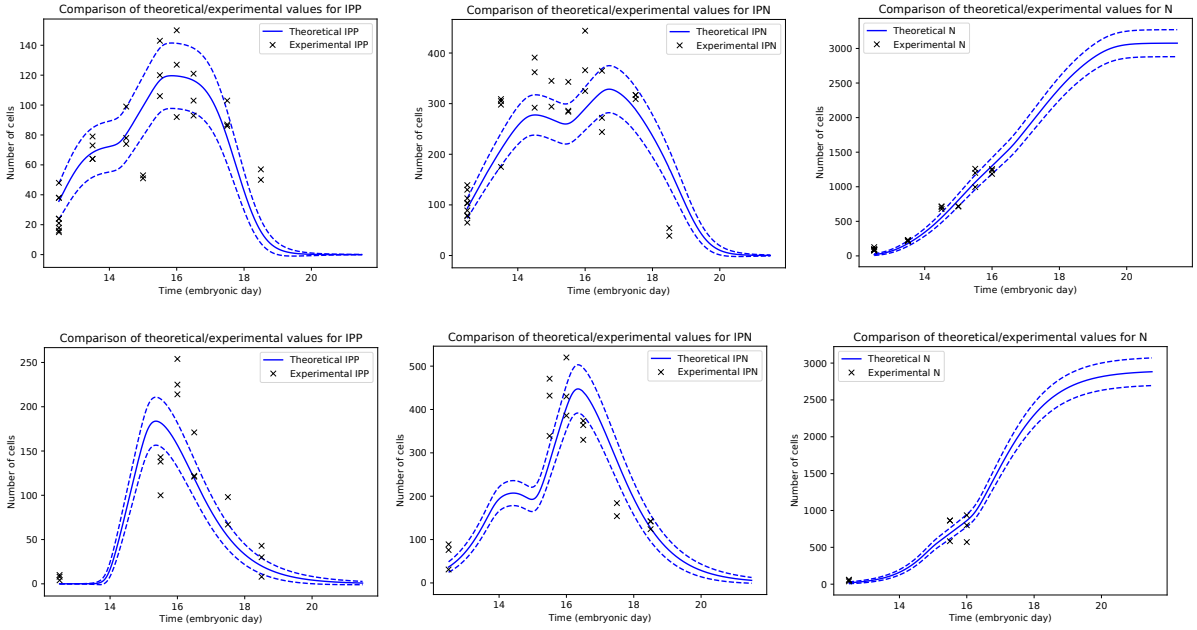

Figure 5: Fitting of progenitor and neuron dynamics to experimental data. *Upper panels: wild-type mice. Lower panels: mutant mice. From left to right: numbers of IPPs, IPNs and neurons. Crosses: experimental datapoints. Solid blue lines: computed model expectations. Dashed blue lines : confidence intervals drawn from computed standard deviations.*

Obviously, the expectations of the stochastic model outputs fit the experimental data in the same way as the deterministic model (see Figures 5 and 6 in [23]). Especially, the mutant is characterized by a narrower time window for neurogenesis, which is compensated for by a more intensive outflow from apical progenitors when neurogenesis is "on", so that the total number of neurons is of the same order as in the wild-type case. Moreover, thanks to the theoretical results on the variance, we can also delimit a 95% confidence interval from the standard variation (dashed curves in Figure 5). To do so, we compute the integrals defined in Propositions 1 and 3 with a quadrature rule.
It is worth recalling that fitting all three datasets requires to optimize a multicriterion objective function. Slight discrepancies between the experimental datasets may thus result in moderate

departures of the fitting curves with respect to experimental data. For instance, the WT IPP datapoints at E18.5 lie upper the fitted curves. Increasing the weight of IPP dynamics in the criterion could make the fitted curves closer to these points, but it would be at severe expense of the IPN fitting, whose final decrease pattern would be deteriorated.
Beyond the observation timepoints, the model predicts that a plateau is reached at birth (E19.5) in the neuron number. In the wild-type case, the final number amounts roughly to 3000 ± 250 neurons, hence more than twice the number observed at the last datapoint (≈ 1250 at E16.5). This increase results from IPNs performing neurogenic divisions from E16.5 onward. Among these cells, many originate from IPP cells born from E15.5 (considering the T_{IPP} delay). In other words, the IPP peak mostly contributes to neuron generation after E16.5.

4.3.3 Fitting of neuron layering

Specific optimization is needed for the parameter set $\mathcal{P}$ in the function specifying neuron layering in Equation (6):

$$\mathcal{P} = \{(\Delta_0, \Delta_1, s_\Delta, t_\Delta) \in \mathbb{R}^4 \,|\, \Delta_0 \in [0.55, 0.95], \Delta_1 \in [0.05, 0.45], s_\Delta \in [0.1, 5], t_\Delta \in [12, 18],\ \Delta_0 > \Delta_1\}.$$

Note that adding these parameters does not alter the structural identifiability of the model, which was thoroughly checked in [23] (supplemental material 7[1]), given that neuron layering is an end-up process with no influence on the remaining dynamics, and that we benefit from additional datasets to estimate the parameter values. Note also that for each event, the number of Bernoulli experiences ($n = 2$ for event 2 and $n = 4$ for event 1) is known and we just need to estimate the second parameter of a Binomial law. Difficulties might arise from the time-varying feature of Δ, yet here we handle them thanks to *a priori* biological knowledge expressed as constraints. Namely, we look for p values such that $\Delta_0 \in [0.55, 0.95], \Delta_1 \in [0.05, 0.45], s_\Delta \in [0.1, 5], t_\Delta \in [12, 18]$.
We implemented a genetic algorithm (details in Section 6.5 and pseudo-code in Algorithm 2) to minimize a least-square criterion, defined for all $p \in \mathcal{P}$ as

$$J(p) = \frac{1}{2} \sum_{t_i} \left(\left(\mathbb{E}_p[DL(t_i)] - DL^m_{t_i} \right)^2 + \left(\mathbb{E}_p[UL(t_i)] - UL^m_{t_i} \right)^2 \right). \tag{23}$$

The optimal values are listed in Table 4 and the corresponding changes in UL and DL cell numbers are illustrated on Figure 6, together with the confidence intervals computed from the results of Propositions 5 and 6.

Parameter	Δ_0	Δ_1	s_Δ	t_Δ
Unit	-	-	d^{-1}	d
Wild-Type	0.554	0.266	4.830	12.07
Mutant	0.583	0.266	4.934	12.05

Table 4: Parameter values for neuron layering in the wild-type and mutant cases.

In both the WT and mutant cases, there is a significant difference between the values of Δ_0 and Δ_1, and a rather steep slope around $t = 12$ days, meaning that there are clearly two regimens with

[1] https://bmcbioinformatics.biomedcentral.com/articles/10.1186/s12859-019-3018-8

first a higher probability of generating DL neurons and then a higher probability of generating UL neurons.

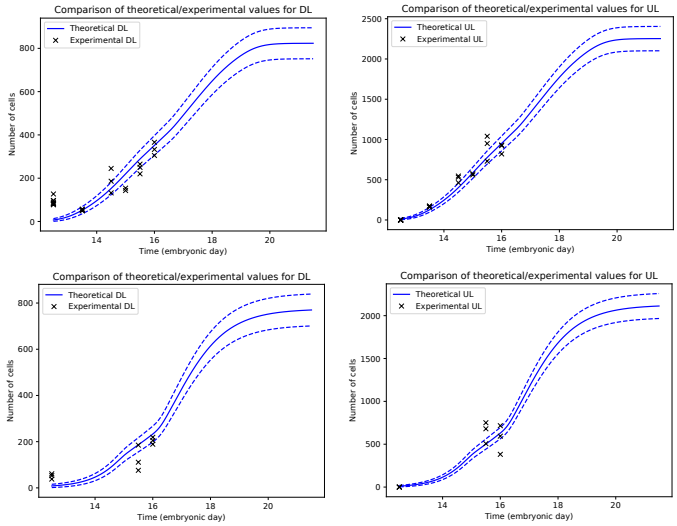

Figure 6: Neuronal distribution into deeper and upper layers. *Upper panels: wild-type mice. Lower panels: mutant mice. Left panels deeper-layer neurons. Right panels : upper-layer neurons. Black crosses: experimental datapoints. Blue lines: fitted values (solid lines: expectations / dashed lines : two standard-deviation intervals).*

The estimated Δ function (see Figure 7 in the Appendix) is consistent with available knowledge on neuron layering. The probability to "choose" a DL location is first higher than that of "choosing" a UL location, and then drops between E12 and E14. Yet, at any time both DLs and ULs can be produced on the individual level, given that the higher asymptote is a little higher than $\frac{1}{2}$ (0.554) and the lower one is far from zero (0.266). This is consistent with both (i) the global trend observed along neurogenesis, with DL created in great part from direct neurogenesis, and as soon as E11.5, while production of UL neurons gets prominent from E13.5/E14.5 [11, 26], and (ii) a remaining of concomitant production of DL and UL [18]. The former was recently confirmed in experiments perturbing the Hippo signaling pathway and resulting in lower intermediate progenitors and upper neurons [26], while the latter is observed in several studies of neuron lineage tracing studies [9, 18]. In particular, in [9], the emergence of neural clones from progenitors stained between E10 and E15 was followed ; all clones were distributed into both the deeper and upper layers, with only a sharp drop in the proportion of DL clones emanating from E15 progenitors. Note also that the (DL) neuron number observed at the earliest time on Figure 6 is due to neurons which arose before the initial time, most probably from direct neurogenesis, while the model predicts the number of new-born neurons in the observation window.
Further comments can be drawn from the (non-monotonic) rate of neuron production in addition to the change in the neuron number (see Figure 8 in the Appendix). First, the bimodal pattern in neuron production mimics the pattern of IPN, which is consistent with the negligible level of direct neurogenesis : all new-born neurons arise from a neurogenic IP. Second, this pattern is reproduced at the level of the UL and DL production rate, with only a difference in amplitude. Another regimen, with the first bump mainly due to DL and the second due to UL could have been compatible with

the total neuron number, yet in our case it can be ruled out since the corresponding parameter set would not fit at all the available data.

5 Discussion

- Comparison between the stochastic and deterministic models
  There is a full consistency between the expectations for cell type numbers in the stochastic model and the corresponding outputs of the deterministic model. As a clear *plus-value*, the stochastic model supplies an estimation of the variance, which could be exploited to define specific error model in data-fitting approaches. There are two few replicates in the current datasets, yet things might improve in a close future. More specifically, more complete datasets assessing the cell numbers on the whole cortex scale have been recently supplied in [14]. Direct exploitation of these datasets in the framework of our model is yet hampered by the lack of distinction between Pax6+Tbr2- and Pax6+Tbr2+, so that Pax6+ cells contain both APs and IPPs, while IPPs are not distinguished from IPN.
  The study with stochastic durations of the cell cycle reveals that a significant variability in the cell cycle alters the pattern of the IP cell numbers along development, and blurs the bimodal pattern observed both in $IPP(t)$ and $IPN(t)$ data and fitted curves. This suggests that the cell cycle duration of progenitors may be rather tightly controlled so that intra-type variability of cell cycle duration be limited.

- Extension to neuron layering
  The results of our fitting study predict that there are more ULs than DLs (with a ratio amounting to ≈ 2.7) at the end of neurogenesis. This is consistent with the recent exhaustive counting of cortex cells [14], where the same markers were used to identify DL and UL (respectively Ctip2 and Stab2), and in contrast with former studies based on sampled countings, where the difference in number between UL and DL is less pronounced [28] or even reversed [8]. Such a discrepancy might be explained at least in part by a bias affecting more severely the counting of upper- (versus deeper-) layer neurons on histological slices retrieved from the cortex at the end of neurogenesis. At this time, indeed, despite of the columnar organization of cortex development, neurons can exit from the observation field, especially in the uppermost part (see Figure 10). Even if this effect is less pronounced in lissencephalic species, as the mouse, compared to gyrencephalic species (see for instance the bottomleft panel of Figure 2 in [6]), it really matters when considering cell dynamics in the developing cortex from a quantitative viewpoint. In addition, some studies used Brn2 rather than Stab2 as an UL-marker, and, even if both markers are supposed to target the same neuron subpopulation, this might add another source of variability.
  Given that the neuron type is in great part dependent on the neuron birth date, in a merely all-or-none manner, the effect of stochastic cycles depend mostly on whether the variability in the cell cycle duration modifies significantly the proportion of neurons born before (or after) the switching time t_Δ compared to the case of constant durations. Actually, with the estimated value of t_Δ, and the mean values of T_{IPP} and T_{IPN}, only neurons arising from event 2 can be affected. In our simulation, this effect was visible with an exponentially distributed duration, with a relatively higher proportion of DL neurons associated with the realization of the shortest cell IPN cycles and anticipated neuron birth (Figure 9).

In the case of mutant mice, the fitting is good for ULs, while there is a discrepancy for the DLs. The issue might come from the importance of patterning defaults along cortex development in *Ftm/Rpgrip1l* mice [3], hence a perturbed architecture of cortical layers. Deleterious mutations in the primary cilium are expected to perturb neurogenesis. Indeed the primary cilium of apical progenitors bathe within the cerebrospinal fluid, whose composition in terms of signaling factors (e.g. Sonic Hedgehog or retinoic acid) changes along development and participate in the control of neurogenesis. An alternative, possibly complementary explanation may be due to changes and/or delays in the differentiation program and expression of DL specific molecular markers such as Ctip2.

- Modeling perspectives
  In the model, the number of cell cycles of IPP remains deterministic. More than two-cell cycle rounds could be encountered on an individual cell basis, yet it seems that such events occur very rarely and hardly alter the dynamics on a population scale.

  A more critical issue is the dynamics of AP, which is still considered implicitly here, from the outflow of daughter cells changing types at the end of an asymmetric division. This is because of the difficulty to number AP cells. Some of them, especially the self-renewing AP, divide from a vertical division plane, so that they exit from the observation field (see Figure 2 in [22] and a schematic illustration in Figure 10). Hence the observed number is a minor bound of the total number. Dedicated numbering studies (as that performed in [14]) as well as mechanistic investigation on AP cell decision making in relation with cell cycle features, as for instance the duration of phase G2 [25], will help in the future to design models with detailed AP dynamics and validate their results from new experimental data.

6 Appendix

6.1 Proof of Theorem 1

We derive here the proof of Theorem 1 as an adaptation to our setting of Theorem 2.1 in [5]. Let $t \geq 0$ and $u \in \mathbb{R}^d$. Following the approach introduced in [5], we have

$$\mathbb{E}\left[e^{i\langle u, X_t\rangle}\right] = \sum_{\nu=0}^{+\infty} \mathbb{E}\left[e^{i\langle u, X_t\rangle}\,;\, Z_t = \nu\right]. \tag{24}$$

The kernel of $(Y_t^{(l)})_{l\in\mathbb{N}^*}$ is L_t, so that we get

$$\mathbb{E}\left[e^{i\langle u, X_t\rangle}\,;\, Z_t = \nu\right] = \int_0^t \int_{s_1}^t \cdots \int_{s_{\nu-1}}^t \int_{\mathbb{R}^d} \cdots \int_{\mathbb{R}^d} \prod_{l=1}^{\nu} e^{i\langle u, y_l\rangle} L_t(s_l, dy_l)$$
$$\cdot \int_t^{+\infty} \frac{dF(s_{\nu+1})}{\overline{F}(s_\nu)} \cdots \frac{dF(s_2)}{\overline{F}(s_1)} dF(s_1),$$

where $\overline{F}(s) = \exp\left(-\int_0^s \lambda(u)du\right)$, $F(s) = 1 - \overline{F}(s)$, and $\frac{dF(s_k)}{\overline{F}(s_{k-1})} = \lambda(s_k)\exp\left(-\int_{s_{k-1}}^{s_k} \lambda(u)du\right) ds_k$ is the stochastic measure associated with arrival time T_{s_k} given $T_{s_{k-1}}$. We denote for all $s \geq 0$ the function $\phi(s) = \frac{1}{\overline{F}(s)} \int_{\mathbb{R}^d} e^{i\langle u, y\rangle} L_t(s, dy)$. Then, we have by permutation, for $a \leq b$ real numbers, $n \in \mathbb{N}^*$,

$$\int_a^b \int_{s_1}^b \dots \int_{s_{n-1}}^b \int_{\mathbb{R}^d} \dots \int_{\mathbb{R}^d} \prod_{l=1}^n e^{i\langle u, y_l\rangle} L_t(s_l, dy_l) \frac{dF(s_n)}{\overline{F}(s_n)} \dots \frac{dF(s_1)}{\overline{F}(s_1)}$$
$$= \int_{a \le s_1 \le \dots \le s_n \le b} \phi(s_1) \dots \phi(s_n) dF(s_n) \dots dF(s_1) = \frac{1}{n!} \left(\int_a^b \phi(s) dF(s) \right)^n.$$

Hence, it comes

$$\mathbb{E}\left[e^{i\langle u, X_t\rangle} \, ; \, Z_t = \nu \right] = \frac{1}{\nu!} \left(\int_0^t \phi(s) dF(s) \right)^\nu \overline{F}(t). \tag{25}$$

Plugging Equation (25) in (24), and summing yields

$$\mathbb{E}\left[e^{i\langle u, X_t\rangle} \right] = \exp\left(\int_0^t \phi(s) dF(s) \right) \overline{F}(t).$$

To end up, we just have to develop ϕ and dF as follows

$$\begin{aligned}\mathbb{E}\left[e^{i\langle u, X_t\rangle} \right] &= \exp\left(\int_0^t \frac{1}{\overline{F}(s)} \int_{\mathbb{R}^d} e^{i\langle u, y\rangle} L_t(s, dy) dF(s) \right) \exp\left(- \int_0^t \lambda(s) ds \right) \\ &= \exp\left(\int_0^t \int_{\mathbb{R}^d} \left(e^{i\langle u, y\rangle} - 1 \right) L_t(s, dy) \lambda(s) ds \right).\end{aligned}$$

□

6.2 Expression of the moments for upper and deeper neurons

Let $t \ge 0$. From the results of Section 3.3, we have that

$$\mathbb{E}[DL(t)] = \mathbb{E}[DL^{(1)}(t - T_{IPP} - T_{IPN})] 1_{t \ge T_{IPP} + T_{IPN}} + \mathbb{E}[DL^{(2)}(t - T_{IPN})] 1_{t \ge T_{IPN}} + \mathbb{E}[DL^{(3)}(t)].$$

Also, given the pairwise independence of $DL^{(1)}(t)$, $DL^{(2)}(t)$ and $DL^{(3)}(t)$ (given by Corollary 2), we have

$$\mathrm{Var}(DL(t)) = \mathrm{Var}(DL^{(1)}(t - T_{IPP} - T_{IPN})) 1_{t \ge T_{IPP} + T_{IPN}} + \mathrm{Var}(DL^{(2)}(t - T_{IPN})) 1_{t \ge T_{IPN}} + \mathrm{Var}(DL^{(3)}(t)).$$

This leads to the following proposition.

Proposition 5. *For all $t \ge 0$,*

$$\begin{aligned}\mathbb{E}[DL(t)] \;=\; & 4 \left(\int_0^{t - T_{IPP} - T_{IPN}} \gamma(s) \beta(s) \Delta(s + T_{IPP} + T_{IPN}) F_{AP}(s) ds \right) 1_{t \ge T_{IPP} + T_{IPN}} \\ & + \; 2 \left(\int_0^{t - T_{IPN}} (1 - \gamma(s)) \, \beta(s) \Delta(s + T_{IPN}) F_{AP}(s) ds \right) 1_{t \ge T_{IPN}} \\ & + \; \int_0^t (1 - \beta(s)) \, \Delta(s) F_{AP}(s) ds,\end{aligned}$$

$$
\begin{aligned}
\mathrm{Var}(DL(t)) &= 12\left(\int_0^{t-T_{IPP}-T_{IPN}} \gamma(s)\beta(s)\left(\Delta(s+T_{IPP}+T_{IPN})\right)^2 F_{AP}(s)ds\right)1_{t\geq T_{IPP}+T_{IPN}} \\
&+ 4\left(\int_0^{t-T_{IPP}-T_{IPN}} \gamma(s)\beta(s)\Delta(s+T_{IPN}+T_{IPN})F_{AP}(s)ds\right)1_{t\geq T_{IPP}+T_{IPN}} \\
&+ 2\left(\int_0^{t-T_{IPN}} (1-\gamma(s))\,\beta(s)\left(\Delta^2+\Delta\right)(s+T_{IPN}+T_{IPN})F_{AP}(s)ds\right)1_{t\geq T_{IPN}} \\
&+ \int_0^t (1-\beta(s))\,\Delta(s)F_{AP}(s)ds.
\end{aligned}
$$

The same approach is used for the moments of $UL(t)$, after introducing the new function $\overline{\Delta} = 1-\Delta$.

Proposition 6. *For all $t \geq 0$,*

$$
\begin{aligned}
\mathbb{E}[UL(t)] &= 4\left(\int_0^{t-T_{IPP}-T_{IPN}} \gamma(s)\beta(s)\overline{\Delta}(s+T_{IPP}+T_{IPN})F_{AP}(s)ds\right)1_{t\geq T_{IPP}+T_{IPN}} \\
&+ 2\left(\int_0^{t-T_{IPN}} (1-\gamma(s))\,\beta(s)\overline{\Delta}(s+T_{IPN}))F_{AP}(s)ds\right)1_{t\geq T_{IPN}} \\
&+ \int_0^t (1-\beta(s))\,\overline{\Delta}(s)F_{AP}(s)ds, \\
\mathrm{Var}(UL(t)) &= 12\left(\int_0^{t-T_{IPP}-T_{IPN}} \gamma(s)\beta(s)\overline{\Delta}(s+T_{IPP}+T_{IPN})^2F_{AP}(s)ds\right)1_{t\geq T_{IPP}+T_{IPN}} \\
&+ 4\left(\int_0^{t-T_{IPP}-T_{IPN}} \gamma(s)\beta(s)\overline{\Delta}(s+T_{IPN}+T_{IPN})F_{AP}(s)ds\right)1_{t\geq T_{IPP}+T_{IPN}} \\
&+ 2\left(\int_0^{t-T_{IPN}} (1-\gamma(s))\,\beta(s)\left(\overline{\Delta}^2+\overline{\Delta}\right)(s+T_{IPN}+T_{IPN})F_{AP}(s)ds\right)1_{t\geq T_{IPN}} \\
&+ \int_0^t (1-\beta(s))\,\overline{\Delta}(s)F_{AP}(s)ds.
\end{aligned}
$$

6.3 Expressions of the moments for upper and deeper neurons in case of stochastic cell cycle durations

Let $(B_k^{(1,i)})_{k\in\mathbb{N}^*,i\in\{1,2\}}$ and $(B_k^{(i)})_{k\in\mathbb{N}^*,i\in\{2,3\}}$ be the stochastic variables introduced in Section 2.4, such that, for any $k \in \mathbb{N}^*$,

$$
\begin{aligned}
B_k^{(1,i)}|T_k, R_k^{(1,i)}, S_k &= \mathrm{Binom}(2, \Delta(T_k + R_k^{(1,i)} + S_k)) \text{ for } i \in \{1,2\}, \\
B_k^{(2)}\,|\,T_k, R_k^{(2)} &= \mathrm{Binom}(2, \Delta(T_k + R_k^{(2)})), \\
B_k^{(3)}|T_k &= \mathrm{Binom}(1, \Delta(T_k)).
\end{aligned}
$$

For all $t \geq 0$, we have

$$DL(t) = \sum_{k=1}^{Z_t^{AP}} \Big(1_{Y_k=1} \left(1_{T_k+S_k+R_k^{(1,1)} \le t} B_k^{(1,1)} + 1_{T_k+S_k+R_k^{(1,2)} \le t} B_k^{(1,2)} \right) + 1_{Y_k=2} 1_{T_k+R_k^{(2)} \le t} B_k^{(2)} + 1_{Y_k=3} B_k^{(3)} \Big), \tag{26}$$

and

$$UL(t) = \sum_{k=1}^{Z_t^{AP}} \Big(1_{Y_k=1} \left(1_{T_k+S_k+R_k^{(1,1)} \le t} (2 - B_k^{(1,1)}) + 1_{T_k+S_k+R_k^{(1,2)} \le t} (2 - B_k^{(1,2)}) \right) + 1_{Y_k=2} 1_{T_k+R_k^{(2)} \le t} (2 - B_k^{(2)}) + 1_{Y_k=3} (1 - B_k^{(3)}) \Big). \tag{27}$$

Using Equations (26) and (27), we obtain the following proposition.

Proposition 7. *For all $t \ge 0$, we have*

$$\begin{aligned}
\mathbb{E}[DL(t)] &= 4 \int_0^t \gamma(u)\beta(u) \left(\int_0^{t-u} \mu_{IPN} \left(\Delta \left([u+s, t] \right) \right) d\mu_{IPP}(s) \right) F_{AP}(u) du \\
&\quad + 2 \int_0^t \left(1 - \gamma(s) \right) \beta(s) \mu_{IPN} \left(\Delta \left([s, t] \right) \right) F_{AP}(s) ds \\
&\quad + \int_0^t (1 - \beta(s)) \Delta(s) F_{AP}(s) ds, \\
\mathbb{E}[UL(t)] &= 4 \int_0^t \gamma(u)\beta(u) \left(\int_0^{t-u} \mu_{IPN} \left(\overline{\Delta} \left([u+s, t] \right) \right) d\mu_{IPP}(s) \right) F_{AP}(u) du \\
&\quad + 2 \int_0^t \left(1 - \gamma(s) \right) \beta(s) \mu_{IPN} \left(\overline{\Delta} \left([s, t] \right) \right) F_{AP}(s) ds \\
&\quad + \int_0^t (1 - \beta(s)) \overline{\Delta}(s) F_{AP}(s) ds.
\end{aligned}$$

and

$$\begin{aligned}
\mathrm{Var}(DL(t)) &= 8\int_0^t \gamma(u)\beta(u)\left(\int_0^{t-u}\left(\mu_{IPN}([u+s,t])\right)^2 d\mu_{IPP}(s)\right)F_{AP}(u)du \\
&+ 4\int_0^t \gamma(u)\beta(u)\left(\int_0^{t-u}\mu_{IPN}\left(\left(\Delta+\Delta^2\right)([u+s,t])\right)\right)F_{AP}(u)du \\
&+ 2\int_0^t (1-\gamma(s))\,\beta(s)\mu_{IPN}\left(\left(\Delta+\Delta^2\right)([s,t])\right)F_{AP}(s)ds \\
&+ \int_0^t (1-\beta(s))\Delta(s)F_{AP}(s)ds, \\
\mathrm{Var}(UL(t)) &= 8\int_0^t \gamma(u)\beta(u)\left(\int_0^{t-u}\left(\mu_{IPN}\left(\Delta([u+s,t])\right)\right)^2 d\mu_{IPP}(s)\right)F_{AP}(u)du \\
&+ 4\int_0^t \gamma(u)\beta(u)\left(\int_0^{t-u}\mu_{IPN}\left(\left(\overline{\Delta}+\overline{\Delta}^2\right)([u+s,t])\right)\right)F_{AP}(u)du \\
&+ 2\int_0^t (1-\gamma(s))\,\beta(s)\mu_{IPN}\left(\left(\overline{\Delta}+\overline{\Delta}^2\right)([s,t])\right)F_{AP}(s)ds \\
&+ \int_0^t (1-\beta(s))\overline{\Delta}(s)F_{AP}(s)ds.
\end{aligned}$$

We provide the proof for DL. The results for UL are obtained in the same way by changing Δ into $\overline{\Delta}$ in the Binomial laws.

Proof. Let $t \geq 0$. We introduce

$$\begin{aligned}
DL^{(1)}(t) &= \sum_{k=1}^{Z_t^{AP}} 1_{Y_k=1}\left(1_{T_k+S_k+R_k^{(1,1)}\leq t}B_k^{(1,1)} + 1_{T_k+S_k+R_k^{(1,2)}\leq t}B_k^{(1,2)}\right) =: \sum_{k=1}^{Z_t^{AP}} A_t^{(k,1)}, \\
DL^{(2)}(t) &= \sum_{k=1}^{Z_t^{AP}} 1_{Y_k=2}1_{T_k+R_k^{(2)}\leq t}B_k^{(2)} =: \sum_{k=1}^{Z_t^{AP}} A_t^{(k,2)}, \\
DL^{(3)}(t) &= \sum_{k=1}^{Z_t^{AP}} 1_{Y_k=3}B_k^{(3)} =: \sum_{k=1}^{Z_t^{AP}} A_t^{(k,3)}.
\end{aligned}$$

We proceed in the same way as in Section 6.2 : we first compute the expectation and variance of each $DL^{(i)}(t)$, from which we deduce by direct summing the expectation of $DL(t)$, and, thanks to Corollary 2, the variance of $DL(t)$, as expressed in Proposition 7.
Denote $L_t^{(3)}$, the kernel associated with the stochastic variables $\left(A_t^{(k,3)}\right)_{k\in[\![1,Z_t^{AP}]\!]}$. $L_t^{(3)}$ is obtained as the result of a Bernoulli experience. Then, for all $s \geq 0$,

$$L_t^{(3)}(s,dy) = (1-\beta(s))\Delta(s)\delta_1(dy) + (1-(1-\beta(s))\Delta(s))\,\delta_0(dy).$$

The direct application of Corollary 1 gives

$$\mathbb{E}[DL^{(3)}(t)] = \mathrm{Var}\left(DL^{(3)}(t)\right) = \int_0^t (1-\beta(s))\Delta(s)F_{AP}(s)ds.$$

We denote $L_t^{(2)}$ the kernel associated with the stochastic variables $\left(A_t^{(k,2)}\right)_{k\in[\![1,Z_t^{AP}]\!]}$. We can compute $L_t^{(2)}$, for all $i \in \{1,2\}$, $k \in [\![1, Z_t^{AP}]\!]$, as

$$\begin{aligned}L_t^{(2)}\left(T_k,\{i\}\right) = \mathbb{P}[A_t^{(k,2)} = i \,|\, T_k] &= \mathbb{P}[Y_k = 2, T_k + R_k^{(2)} \le t, B_k^{(2)} = i \,|\, T_k] \\ &= \left(1-\gamma(T_k)\right)\beta\left(T_k\right)\int_0^{t-T_k}\binom{2}{i}\Delta(T_k+r)^i\left(1-\Delta(T_k+r)\right)^{2-i}d\mu_{IPN}(r).\end{aligned}$$

Hence, applying again Corollary 1

$$\begin{aligned}\mathbb{E}[DL^{(2)}(t)] &= \int_0^t\left(2\int_0^{t-s}\Delta(s+r)^2 d\mu_{IPN}(r) + \int_0^{t-s}2\Delta(s+r)(1-\Delta(s+r))d\mu_{IPN}(r)\right) \\ &\quad\times\left(1-\gamma(s)\right)\beta(s)F_{AP}(s)ds \\ &= 2\int_0^t\left(\int_0^{t-s}\Delta(s+r)d\mu_{IPN}(r)\right)\left(1-\gamma(s)\right)\beta(s)F_{AP}(s)ds \\ &= 2\int_0^t\mu_{IPN}\left(\Delta\left([s,t]\right)\right)\left(1-\gamma(s)\right)\beta(s)F_{AP}(s)ds,\end{aligned}$$

$$\begin{aligned}\mathrm{Var}(DL^{(2)}(t)) &= \int_0^t\left(4\int_0^{t-s}\Delta(s+r)^2 d\mu_{IPN}(r) + \int_0^{t-s}2\Delta(s+r)(1-\Delta(s+r))d\mu_{IPN}(r)\right) \\ &\quad\times\left(1-\gamma(s)\right)\beta(s)F_{AP}(s)ds \\ &= 2\int_0^t\left(\int_0^{t-s}\left(\Delta+\Delta^2\right)(s+r)d\mu_{IPN}(r)\right)\left(1-\gamma(s)\right)\beta(s)F_{AP}(s)ds \\ &= 2\int_0^t\mu_{IPN}\left(\left(\Delta+\Delta^2\right)\left([s,t]\right)\right)\left(1-\gamma(s)\right)\beta(s)F_{AP}(s)ds.\end{aligned}$$

We do not proceed as straightforward for $\left(A_t^{(k,1)}\right)_{k\in[\![1,Z_t^{AP}]\!]}$, to alleviate the computation of the expectation. We rather introduce the filtrations $(\mathcal{F}_s)_{s\ge0}$ and $(\mathcal{G}_s)_{s\ge0}$, such that for all $s \ge 0$

$$\begin{aligned}\mathcal{F}_s &= \sigma\left(\left(Z_r^{AP}\right)_{r\le s}, (T_j)_{j\in[\![1,Z_s^{AP}]\!]}, (Y_j)_{j\in[\![1,Z_s^{AP}]\!]}\right), \\ \mathcal{G}_s &= \sigma\left(\left(Z_r^{AP}\right)_{r\le s}, (T_j)_{j\in[\![1,Z_s^{AP}]\!]}, (R_j^{(1,i)})_{j\in\mathbb{N}^*,i\in\{1,2\}}, (S_j)_{j\in\mathbb{N}^*}, (Y_j)_{j\in[\![1,Z_s^{AP}]\!]}\right).\end{aligned}$$

For all $k \in \{1,2,\dots,Z_t^{AP}\}$, as the two terms in $A_t^{(k,1)}$ have the same distribution conditionally to $\mathcal{F}_t$, we obtain

$$\begin{aligned}\mathbb{E}\left[A_t^{(k,1)}|\mathcal{F}_t\right] &= 2\mathbb{E}\left[1_{Y_k=1}1_{T_k+S_k+R_k^{(1,1)}\le t}B_k^{(1,1)}|\mathcal{F}_t\right] \\ &= 21_{Y_k=1}\mathbb{E}\left[1_{T_k+S_k+R_k^{(1,1)}\le t}B_k^{(1,1)}|\mathcal{F}_t\right] \\ &= 21_{Y_k=1}\mathbb{E}\left[1_{T_k+S_k+R_k^{(1,1)}\le t}\mathbb{E}\left[B_k^{(1,1)}|\mathcal{G}_t\right]|\mathcal{F}_t\right].\end{aligned}$$

Then, as $B_k^{(1,1)}|T_k, S_k, R_k^{(1,1)}$ follows a Binomial distribution, we have

$$\begin{aligned}\mathbb{E}[A_t^{(k,1)}|\mathcal{F}_t] &= 41_{Y_k=1}\mathbb{E}\left[\Delta(T_k+S_k+R_k^{(1,1)})1_{T_k+S_k+R_k^{(1,1)}\leq t}|\mathcal{F}_t\right] \\ &= 41_{Y_k=1}\int_{\{(r,s)\in\mathbb{R}^2|r+s\in[0,t-T_k]\}}\Delta(T_k+s+r)d(\mu_{IPN}\times\mu_{IPP})(r,s),\end{aligned}$$

and then using the definition of $d(\mu_{IPN}\times\mu_{IPP})(r,s)$

$$\begin{aligned}\mathbb{E}[A_t^{(k,1)}|\mathcal{F}_t] &= 41_{Y_k=1}\int_0^{t-T_k}\left(\int_0^{t-T_k-s}\Delta(T_k+s+r)d\mu_{IPN}(r)\right)d\mu_{IPP}(s) \\ &= 41_{Y_k=1}\int_0^{t-T_k}\mu_{IPN}\left(\Delta([T_k+s,t])\right)d\mu_{IPP}(s).\end{aligned}$$

Hence, we have

$$\begin{aligned}\mathbb{E}[DL^{(1)}|\mathcal{F}_t] &= \sum_{k=1}^{Z_{AP}(t)}\mathbb{E}[A_t^{(k,1)}|\mathcal{F}_t] \\ &= 4\sum_{k=1}^{Z_{AP}(t)}\left(1_{Y_k=1}\int_0^{t-T_k}\mu_{IPN}\left(\Delta([T_k+s,t])\right)d\mu_{IPP}(s)\right).\end{aligned}$$

From the expression above, we see that $(\mathbb{E}[DL^{(1)}|\mathcal{F}_s])_{s\geq 0}$ is a compound Poisson process whose kernel is given by

$$\begin{aligned}L_t(T_k,dy) &= \gamma(T_k)\beta(T_k)\delta_{4\left(\int_0^{t-T_k}\mu_{IPN}(\Delta([T_k+s,t]))d\mu_{IPP}(s)\right)}(dy) \\ &\quad + (1-\gamma(T_k)\beta(T_k))\,\delta_0(dy).\end{aligned}$$

Arriving here we can apply Corollary 1 and obtain

$$\begin{aligned}\mathbb{E}\left[\mathbb{E}[DL^{(1)}(t)|\mathcal{F}_t]\right] &= 4\int_0^t\gamma(u)\beta(u)\left(\int_0^{t-u}\mu_{IPN}\left(\Delta\left([u+s,t]\right)\right)d\mu_{IPP}(s)\right)F_{AP}(u)du \\ &= \mathbb{E}[DL^{(1)}(t)].\end{aligned}$$

For the variance of $DL^{(1)}(t)$, we cannot use the same strategy to alleviate the computation, and we have to handle $L_t^{(1)}$. Using Corollary 1, we have

$$\begin{aligned}\mathrm{Var}(DL^{(1)}(t)) &= \int_0^t\left(\int_{\mathbb{R}}y^2L_t^{(1)}(u,dy)\right)F_{AP}(u)ds \\ &= \sum_{i=1}^4 i^2\int_0^t\mathbb{P}\left[1_{T_1+S_1+R_1^{(1,1)}\leq t}B_1^{(1,1)}+1_{T_1+S_1+R_1^{(1,2)}\leq t}B_1^{(1,2)}=i\,|\,T_1=u\right] \\ &\quad\times\mathbb{P}\left[Y_1=1\,|\,T_1=u\right]F_{AP}(u)du \\ &= \int_0^t\left(\int_0^{t-u}\mathbb{E}[Y_{s,u}^2]d\mu_{IPP}(s)\right)\gamma(u)\beta(u)F_{AP}(u)du,\end{aligned}$$

where

$$Y_{s,u} = 1_{R^{(1)} \leq t-s-u} B^{(1)}_{s,u} + 1_{R^{(2)} \leq t-s-u} B^{(2)}_{s,u},$$

and $\left(R^{(1)}, B^{(1)}_{s,u}\right)$ and $\left(R^{(2)}, B^{(2)}_{s,u}\right)$ are two independent pairs of random variables, such that, for $i \in \{1,2\}$, $R^{(i)}$ is distributed according to the probability measure μ_{IPN}, and

$$B^{(i)}_{s,u} | R^{(i)} \sim \text{Binom}\left(2, \Delta(u+s+R^{(i)})\right).$$

We just need now to develop the terms of $Y_{s,u}$. First, as the pairs $\left(R^{(1)}, B^{(1)}_{s,u}\right)$ and $\left(R^{(2)}, B^{(2)}_{s,u}\right)$ are independent from each other, and follow the same distribution, we have

$$\begin{aligned}
\mathbb{E}[Y^2_{s,u}] &= \mathbb{E}\left[1_{R^{(1)} \leq t-s-u} \left(B^{(1)}_{s,u}\right)^2\right] + \mathbb{E}\left[1_{R^{(2)} \leq t-s-u} \left(B^{(2)}_{s,u}\right)^2\right] + 2\mathbb{E}\left[1_{R^{(1)} \leq t-s-u} 1_{R^{(2)} \leq t-s-u} B^{(1)}_{s,u} B^{(2)}_{s,u}\right] \\
&= 2\mathbb{E}\left[1_{R^{(1)} \leq t-s-u} \left(B^{(1)}_{s,u}\right)^2\right] + 2\mathbb{E}\left[1_{R^{(1)} \leq t-s-u} B^{(1)}_{s,u}\right]^2.
\end{aligned}$$

Using the fact that $B^{(1)}_{s,u} \,|\, R^{(1)}$ follows a Binomial distribution

$$\begin{aligned}
\mathbb{E}[Y^2_{s,u}] &= 2\int_0^{t-s-u} \mathbb{E}\left[\left(B^{(1)}_{s,u}\right)^2 \,|\, R^{(1)} = r\right] d\mu_{IPN}(r) + 2\left(\int_0^{t-s-u} \mathbb{E}\left[B^{(1)}_{s,u} \,|\, R^{(1)} = r\right] d\mu_{IPN}(r)\right)^2 \\
&= 4\int_0^{t-s-u} \Delta(r+s+u)\left(1 - \Delta(r+s+u)\right) d\mu_{IPN}(r) + 8\int_0^{t-s-u} \Delta(r+s+u)^2 d\mu_{IPN}(r) \\
&\quad + 8\left(\int_0^{t-s-u} \Delta(r+s+u) d\mu_{IPN}(r)\right)^2,
\end{aligned}$$

which can be rewritten as

$$\begin{aligned}
\mathbb{E}[Y^2_{s,u}] &= 4\int_0^{t-s-u} \left(\Delta(r+s+u) + \Delta^2(r+s+u)\right) d\mu_{IPN}(r) + 8\left(\int_0^{t-s-u} \Delta(r+s+u) d\mu_{IPN}(r)\right)^2 \\
&= 4\mu_{IPN}\left(\left(\Delta + \Delta^2\right)([u+s,t])\right) + 8\left(\mu_{IPN}([u+s,t])\right)^2.
\end{aligned}$$

We finally get

$$\begin{aligned}
\text{Var}(DL^{(1)}(t)) &= 8\int_0^t \gamma(s)\beta(s)\left(\int_0^{t-u} \left(\mu_{IPN}\left(\Delta([u+s,t])\right)\right)^2 d\mu_{IPP}(s)\right) F_{AP}(u)du \\
&\quad + 4\int_0^t \gamma(s)\beta(s)\left(\int_0^{t-u} \mu_{IPN}\left(\left(\Delta + \Delta^2\right)([u+s,t])\right)\right) F_{AP}(u)du.
\end{aligned}$$

We conclude the proof of Proposition 7 by the final summing step. □

6.4 Formulation of the time-varying intensities with default parameter values

Figure 7 displays the graphs of the different intensity functions of the model, F_{AP}, γ and Δ, with the optimized parameter values gathered in Table 2.

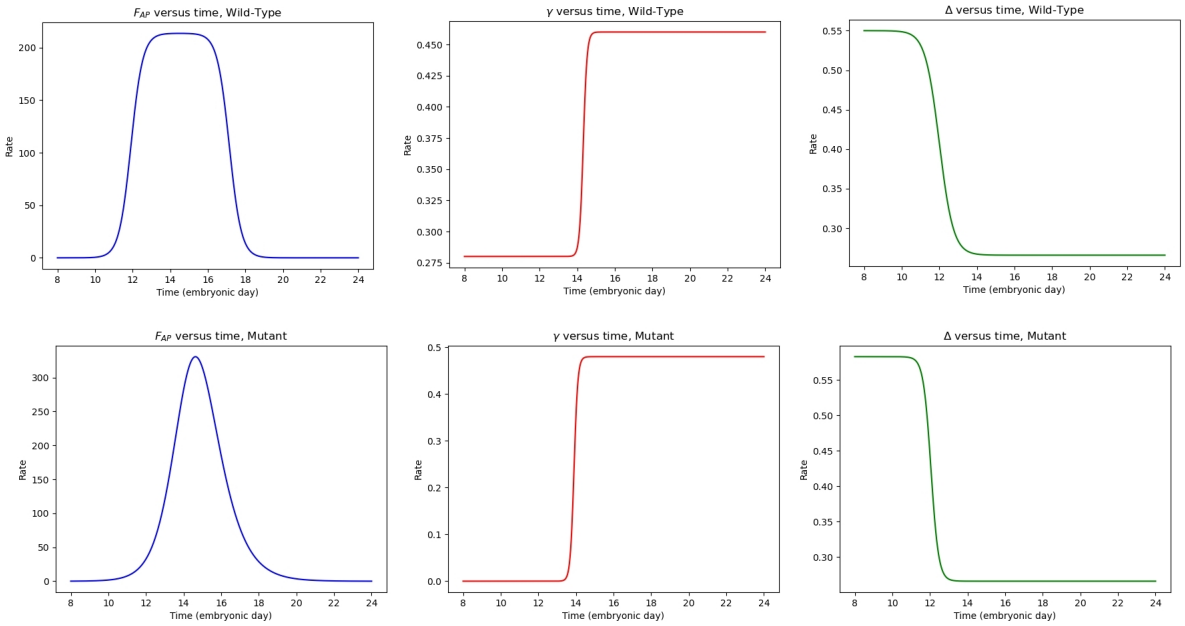

Figure 7: Graphs of F_{AP}, γ and Δ. *Top panels: wild-type mice. Bottom panels: mutant mice.*

6.5 Parameter optimization for neuron layering

To optimize criterion J (defined in (23)) and find the optimal values of $\mathcal{P}$, we implemented a genetic algorithm.

First we discretized the parameter space from $\mathcal{P}$ into $4 \times (2^n + 1)$ points, where $n \in \mathbb{N}^*$, and obtain the following set

$$\mathcal{P}_n = \left\{ \left(0.55 + \frac{0.4}{2^n} k_1, 0.05 + \frac{0.4}{2^n} k_2, 0.1 + \frac{4.9}{2^n} k_3, 12 + \frac{6}{2^n} k_4 \right) \;\middle|\; (k_1, k_2, k_3, k_4) \in [\![0, 2^n]\!]^4 \right\}.$$

The integers k_1, k_2, k_3 and k_4 are encoded as a single binary vector of size $4(n+1)$, such that for all $i \in \{1, 2, 3, 4\}$, each k_i value spans the $(i-1) \times (n+1) + 1 \to i \times (n+1)$ coordinate range.

The parameters are selected from a population of constant size $N \in \mathbb{N}^*$, in which each individual is characterized by a different k_{i_s} vector. At each iteration, the best fitted n_e individuals are retained ($n_e \in \mathbb{N}$, the fitness criterion is $-J$). Among the other $N - n_e$ individuals, n_m undergo parameter mutation, i.e. a proportion $\mu \in [0, 1]$ of the binary values are flipped. Finally, n_b individuals are removed and replaced by new-born individuals ($n_b \in \mathbb{N}$), whose parents are selected in the whole population with probability $\ell(p_i) = \frac{\frac{1}{J(p_i)}}{\sum_{k=1}^{N} \frac{1}{J(p_k)}}$ (for all $i \in [\![1, N]\!]$, $p_i \in \mathcal{P}^n$ is the parameter of the $i-th$ individual in the population). The new-born individuals inherit from the parameter vector of one of their two parents.

Algorithm 2 Pseudo-code of the genetic algorithm.

population $\leftarrow$ population$_{\text{init}}$
fitness $\leftarrow -J$(population)
for $g = 1, \ldots, G_{max}$ **do**
    population $\leftarrow$ population[argsortmax(fitness)]
    fitness $\leftarrow$ fitness[argsortmax(fitness)]
    $p_{\text{reprod}} \leftarrow \ell$(population)
    newpop $\leftarrow$ shuffle(population[n_e : end])
    for $i = 1, \ldots n_b$ **do**
        parent$_1 \leftarrow$ choice(population, p_{reprod})
        parent$_2 \leftarrow$ choice(population, p_{reprod})
        newpop[i] $\leftarrow$ reproduct(parent$_1$, parent$_2$)
    for $i = n_b + 1, \ldots n_m$ **do**
        for $j = 1 \ldots \lfloor 4\mu(n+1) \rfloor$ **do**
            flip (newpop[i][random$(1, 4n)$])
    population[n_e : end] $\leftarrow$ newpop
    fitness $\leftarrow -J$(population)
return population[argmax(fitness)]

N	G_{max}	n	n_e	n_b	n_m	μ
50	100	14	4	20	26	0.5

Table 5: Values of the meta-parameters for the genetic algorithm.

The numbers of DLs and ULs obtained with the optimal parameter sets are shown in Figure 6 in Section 4.3.3. Further information (see body text) are provided by looking at the instantaneous change in the total number of neurons and the distribution into DLs and ULs, illustrated on Figure 8.

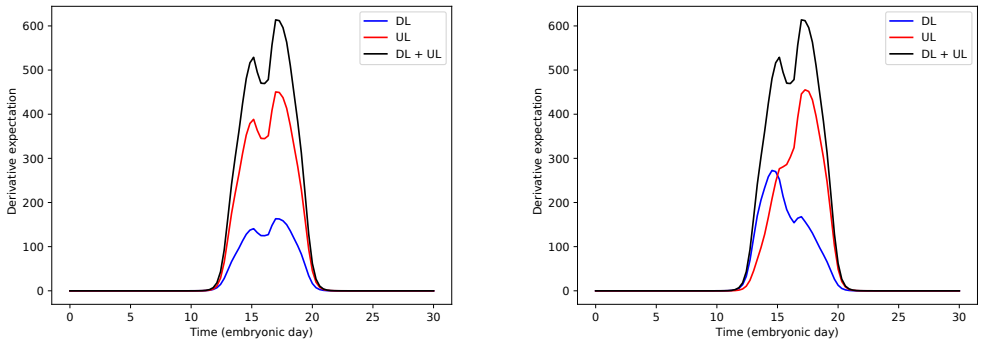

Figure 8: Instantaneous changes in neuron numbers in WT mice. *Instantaneous change in the total neuron number (black lines), and respective contribution of DLs (blue lines) and ULs (red lines). Left panel: regimen observed with the optimized parameter values. Right panel: alternative regimen with different DL/UL distribution yet identical total neuron production.*

6.6 Stochastic cell cycle durations and neuron layering

Figure 9 displays the difference in the DL and UL neuron numbers observed for different distributions of the cell cycle duration (Gamma, Beta or Exponential law) and with respect to a deterministic (constant) duration.

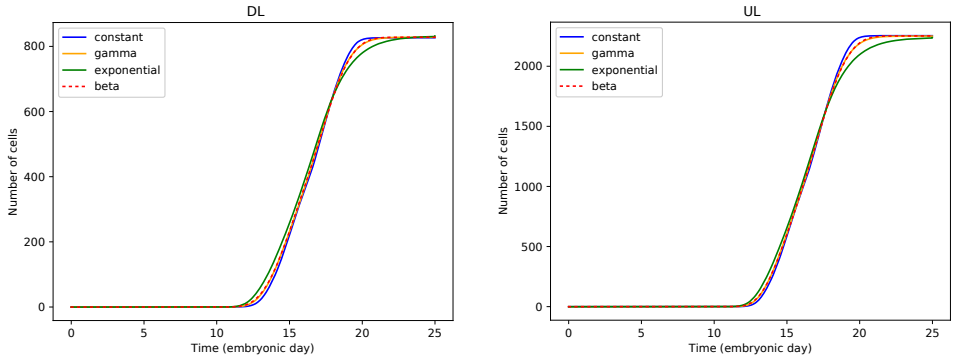

Figure 9: Mean of upper- and deeper-layer neurons for different cell cycle distributions. *Left panels: deeper-layer neurons. Right panels: upper-layer neurons. On each panel, the expectation is assessed by the empirical mean computed over 500 stochastic trajectories, and the choice of the distribution is color-encoded (red lines: Beta distribution. green lines: Exponential distribution, yellow lines: Gamma distribution). For sake of comparison, the deterministic outputs are also displayed (blue lines).*

6.7 Bias in cell number counting from histological slices

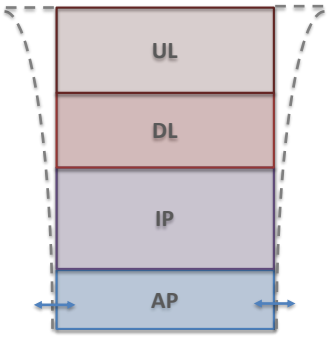

Figure 10: Schematic representation of an histological slice. *The relative location of the cell types are shown, from the apical most cells (AP) lining the cerebral ventricle to the most superficial neurons (UL). The grey dashed lines delimit the possible enlargement of the area containing all neurons emanating from a same row of AP, while the horizontal double arrows indicate the AP leakage from the imaging field due to cells dividing along a vertical plane.*

The columnar anatomical organization of the cortex ensues from the mostly vertical pattern of cortex development. This is why 2D coronal slices are well informative to investigate the dynamics of progenitor dynamics, and especially intermediate progenitors. Yet, one has to be aware of two

possible biases (Figure 10). First, at the end of neurogenesis, neurons may exit from the view field (see top part of Figure 10) ; the cell density is lower for neurons, whose cell endings occupy a relatively great amount of space. Second, apical progenitors at the bottom may exit the field radially after a cell division, depending on the orientation of the division plane.

References

[1] D. Applebaum, B.V.R. Bhat, J. Kustermans, J.M. Lindsay, M. Schuermann, and Franz U. *Quantum Independent Increment Processes I.* Springer, 2005.

[2] Y. Arai, J.N. Pulvers, C Haffner, B. Schilling, I. Nusslein, F. Calegari, and W.B. Huttner. Neural stem and progenitor cells shorten S-phase on commitment to neuron production. *Nat. Commun.*, 2:154, 2011.

[3] L. Besse, M. Neti, I. Anselme, C. Gerhardt, U. Rüther, C. Laclef, and S. Schneider-Maunoury. Primary cilia control telencephalic patterning and morphogenesis via Gli3 proteolytic processing. *Development*, 138(10):2079–2088, 2011.

[4] J.R. Brannan and W.E. Boyce. Spatially localized interactive neural populations—I. a mathematical model. *Bull. Math. Biol.*, 43:427–446, 1981.

[5] C.S. Chen and T.H. Savits. Some remarks on compound nonhomogeneous Poisson processes. *Statist. Probab. Lett.*, 17(3):179–187, 1993.

[6] V. Fernández, C. Llinares-Benadero, and V. Borrell. Cerebral cortex expansion and folding: what have we learned? *EMBO J.*, 35(10):1021–1044, 2016.

[7] M. Florio and W.B. Huttner. Neural progenitors, neurogenesis and the evolution of the neocortex. *Development*, 141(11):2182–2194, 2014.

[8] B. Freret-Hodara, Y. Cui, A. Griveau, L. Vigier, Y. Arai, J. Touboul, and A. Pierani. Enhanced abventricular proliferation compensates cell death in the embryonic cerebral cortex. *Cereb. cortex*, 27(10):1–18, 2016.

[9] P. Gao, M.P. Postiglione, T.G. Krieger, L. Hernandez, C. Wang, Z. Han, C. Streicher, E. Papusheva, R. Insolera, K. Chugh, O. Kodish, K. Huang, B.D. Simons, L. Luo, S. Hippenmeyer, and S.H. Shi. Deterministic progenitor behavior and unitary production of neurons in the neocortex. *Cell*, 159(4):775–788, 2014.

[10] C.R. Gerfen, M.N. Economo, and J. Chandrashekar. Long distance projections of cortical pyramidal neurons. *J. Neurosci. Res.*, 96(9):1467–1475, 2018.

[11] L.C. Greig, M.B. Woodworth, M.J. Galazo, H. Padmanabhan, and J.D. Macklis. Molecular logic of neocortical projection neuron specification, development and diversity. *Nat. Rev. Neurosci.*, 14(11):755–769, 2013.

[12] L.C. Hsu, S. Nam, Y. Cui, C.P. Chang, C.F. Wang, H.C. Kuo, J.D. Touboul, and S.J. Chou. Lhx2 regulates the timing of b-catenin-dependent cortical neurogenesis. *Proc. Natl. Acad. Sci. U.S.A.*, 112(39):199–204, 2015.

[13] J.P. Huelsenbeck, B. Larget, and D. Swofford. A compound Poisson process for relaxing the molecular clock. *Genetics*, 154(4):1879–1892, 2000.

[14] T. Jungas, M. Joseph, M.-A. Fawal, and A. Davy. Population dynamics and neuronal polyploidy in the developing neocortex. *Cereb. Cortex Commun.*, 1(1):tgaa063, 2020.

[15] S.R. Kegler. Applying the compound Poisson process model to the reporting of injury-related mortality rates. *Epidemiol. Perspect. Innov.*, 4(1):1–9, 2007.

[16] A. Kriegstein and A. Alvarez-Buylla. The glial nature of embryonic and adult neural stem cells. *Annu. Rev. Neurosci.*, 32:149–184, 2009.

[17] G. Last and M. Penrose. Compound Poisson Processes. In *Lectures on the Poisson Process*, Institute of Mathematical Statistics Textbooks, pages 153–165. Cambridge University Press, Cambridge, 2017.

[18] A. Llorca, G. Ciceri, R. Beattie, F. K. Wong, G. Diana, E. Serafeimidou-Pouliou, M. Fernández-Otero, C. Streicher, S.J. Arnold, M. Meyer, S. Hippenmeyer, M. Maravall, and O. Marin. A stochastic framework of neurogenesis underlies the assembly of neocortical cytoarchitecture. *Elife*, 8:e51381, 2019.

[19] M. Manuel, K.B. Tan, Z. Kozic, M. Molinek, T.S. Marcos, M.F.A. Razak, D. Dobolyi, R. Dobie, B.E.P. Henderson, N.C. Henderson, W.K. Chan, M.I. Daw, J.O. Mason, and D.J. Price. Pax6 limits the competence of developing cerebral cortical cells to respond to inductive intercellular signals. *PLoS Biol.*, 20(9):e3001563, 2022.

[20] S.J. Nelson. A stochastic model of the effects of ionizing radiation on mammalian cells in vitro. *Bull. Math. Biol.*, 46(3):423–446, 1984.

[21] J. Neyman and P.S. Puri. A structural model of radiation effects in living cells. *Proc. Natl. Acad. Sci. U.S.A.*, 73(10):3360–3363, 1976.

[22] J.T. Paridaen and W.B Huttner. Neurogenesis during development of the vertebrate central nervous system. *EMBO Rep.*, 15(4):351–364, 2014.

[23] M. Postel, A. Karam, G. Pézeron, S. Schneider-Maunoury, and F. Clément. A multiscale mathematical model of cell dynamics during neurogenesis in the mouse cerebral cortex. *BMC Bioinformatics*, 20(470), 2019.

[24] P. Puig and J.F. Barquinero. An application of compound Poisson modelling to biological dosimetry. *Proc. A.*, 467(2127):897–910, 2010.

[25] M. Roussat, T. Jungas, C. Audouard, S. Omerani, F. Medevielle, E. Agius, A. Davy, F. Pituello, and S. Bel-Vialar. Control of G2 phase duration by CDC25B modulates the switch from direct to indirect neurogenesis in the neocortex. *J. Neurosci.*, 43(7):1154–1165, 2023.

[26] Y.-C. Su, T.-H. Hung, T.-F. Wang, Y.-H. Lee, T.-W. Wang, and J.-Y. Yu. YAP maintains the production of intermediate progenitor cells and upper-layer projection neurons in the mouse cerebral cortex. *Dev. Dyn.*, 251(5):846–863, 2022.

[27] Sukono, H. Juahir, R.A. Ibrahim, M.P.A. Saputra, Y. Hidayat, and I.G. Prihanto. Application of compound Poisson process in pricing catastrophe bonds : A systematic literature review. *Mathematics*, 10(15):2668, 2022.

[28] K. Toma, T. Kumamoto, and C. Hanashima. The timing of upper-layer neurogenesis is conferred by sequential derepression and negative feedback from deep-layer neurons. *J. Neurosci.*, 34(39):13259–13276, 2014.

[29] C. Tomasetti, B. Vogelstein, and G. Parmigiani. Half or more of the somatic mutations in cancers of self-renewing tissues originate prior to tumor initiation. *Proc. Natl. Acad. Sci. U.S.A.*, 110(6):1999–2004, 2013.

[30] M. Voliotis, P. Thomas, R. Grima, and C.G. Bowsher. Stochastic simulation of biomolecular networks in dynamic environments. *PloS Comp. Biol.*, 12(06):1–18, 2016.

[31] R. Yvinec, C. Zhuge, J. Lei, and M.C. Mackey. Adiabatic reduction of a model of stochastic gene expression with jump Markov process. *J. Math. Biol.*, 68:1051–1070, 2014.